

# Primary standards and dosimetry protocols for brachytherapy sources

C G Soares<sup>1</sup>, G Douysset<sup>2</sup> and M G Mitch<sup>1</sup>

<sup>1</sup> National Institute of Standards and Technology, Gaithersburg, MD 20899, USA

<sup>2</sup> CEA, LIST, LNE–Laboratoire National Henri Becquerel, F-91191 Gif-sur-Yvette, France

E-mail: [csoares@nist.gov](mailto:csoares@nist.gov)

Received 13 May 2008, in final form 3 September 2008

Published 20 March 2009

Online at [stacks.iop.org/Met/46/S80](http://stacks.iop.org/Met/46/S80)

## Abstract

Current primary standards for the calibration of both photon and beta particle emitting brachytherapy sources are reviewed. Methods for quality control being used as well as methods of transferring these standards to secondary laboratories and users are also discussed. Finally, dosimetry protocols for brachytherapy sources are described.

## 1. Primary air-kerma strength standards for low-dose rate (LDR) brachytherapy sources

### 1.1. Low-energy x-ray emitting LDR brachytherapy sources

*1.1.1. NIST calibrations of <sup>125</sup>I, <sup>103</sup>Pd and <sup>131</sup>Cs sources.* The calibration of low-energy, x-ray emitting LDR brachytherapy sources is accomplished at the National Institute of Standards and Technology (NIST) using the wide-angle free-air chamber (WAFAC) (Seltzer *et al* 2003). The WAFAC is a cylindrical free-air ionization chamber with a large 8 cm diameter aperture which enables the air-kerma of single sources that emit photons of energies up to 40 keV to be directly realized. The x-rays emergent from the source pass through thin, aluminized polyethylene terephthalate electrodes, and collected charge is measured at two volumes to account for interface effects. Air-kerma strength,  $S_K$  is then calculated using the equation

$$S_K = \left( \frac{\bar{W}}{e} \right) \frac{I_{\text{net}} d^2}{\rho_{\text{air}} V_{\text{eff}}} \prod_i k_i, \quad (1)$$

where  $\bar{W}$  is the mean energy per ion pair expended in air when the initial kinetic energy of a charged particle is completely dissipated,  $e$  is the elemental charge,  $I_{\text{net}}$  is the difference in the ionization current for the large chamber volume and the small chamber volume,  $d$  is the distance from the source to the aperture,  $\rho_{\text{air}}$  is the density of air,  $V_{\text{eff}}$  is the product of the aperture area and the difference in the lengths of the two collecting volumes and  $k_i$  are correction factors. The brachytherapy source is mounted vertically on a plastic post at a distance of 30 cm from the entrance aperture. Located between the source and the aperture is an aluminium filter of

0.08636 mm thickness that absorbs the 4.5 keV fluorescence x-rays from the titanium capsule of the source. These low-energy x-rays are eliminated from the beam as they do not contribute to the dose in water at clinically relevant distances, but could affect the air-kerma measurement. The source is rotated at 1 rpm during measurement to average over any anisotropy around its axis. In a separate set of measurements, the magnitude of such anisotropy for each source is quantified by rotating the source at 45° increments and measuring the ionization current using the large WAFAC volume. An <sup>241</sup>Am source is used to verify the stability of the WAFAC system over time. The expanded uncertainty ( $k = 2$ ) for air-kerma strength calibrations of low-energy LDR sources is equal to  $2(s_I^2 + u_j^2)^{1/2}$ , where  $s_I$  is the standard deviation of the mean of replicate measurements (Type A), and the Type B components of uncertainty are represented by  $u_j$ , where  $u_j = 0.762\%$  for <sup>125</sup>I sources, 0.728% for <sup>103</sup>Pd sources and 0.737% for <sup>131</sup>Cs sources. As an example, table 1 gives the values and uncertainties of the parameters in the  $S_K$  equation for <sup>125</sup>I sources. Over 800 sources of 33 different designs from 18 manufacturers have been calibrated by NIST since 1999.

In addition to the WAFAC air-kerma strength calibration, the responses of several well-ionization chambers of different designs are measured, including two types that are open to the atmosphere and one type with pressurized argon as the counting gas. As secondary standard laboratories that maintain traceability to NIST measurements utilize well chambers, it is important to understand the relationship between well chamber response and WAFAC-measured air-kerma strength. Therefore, the x-ray spectrum emergent from the source along its transverse axis is measured using a high-purity germanium (HPGe) spectrometer. Generally speaking, the value of the

**Table 1.** Values and relative standard uncertainties of parameters used in the determination of air-kerma strength for  $^{125}\text{I}$  brachytherapy seeds using the WAFAC. Estimated relative uncertainties ( $1\sigma$ ) are given in per cent, and include the type A uncertainty  $s_i$  estimated by statistical methods and the type B uncertainty  $u_j$  estimated by other means.

	Value	$s_i/\%$	$u_j/\%$
Net current, $I_{\text{net}}$		$s_I$	0.06
$\bar{W}/e$	33.97 J C $^{-1}$	—	0.15
Air density, $\rho_{\text{air}}$	1.196 mg cm $^{-3}$	—	0.03
Aperture distance, $d$		—	0.24
Effective chamber volume, $V_{\text{eff}}$		0.11	0.01
Decay correction, $k_1$	$T_{1/2} = 59.43$ d	—	0.02
Recombination, $k_2$	<1.004	—	0.05
Attenuation in filter, $k_3$	1.0295	—	0.61
Air attenuation in WAFAC, $k_4$	1.0042	—	0.08
Source–aperture attenuation, $k_5$	1.0125	—	0.24
Inverse-square correction, $k_6$	1.0089	—	0.01
Humidity, $k_7$	0.9982	—	0.07
In-chamber photon scatter, $k_8$	0.9966	—	0.07
Source-holder scatter, $k_9$	0.9985	—	0.05
Electron loss, $k_{10}$	1.0	—	0.05
Aperture penetration, $k_{11}$	0.9999	—	0.02
External photon scatter, $k_{12}$	1.0	—	0.17
Combined uncertainty		$(s_I^2 + 0.762^2)^{1/2}$	

well-chamber response coefficient,  $I/S_K$ , where  $I$  is the well chamber current and  $S_K$  is the air-kerma strength, increases with increasing average energy of the emergent spectrum (see figure 1). However, the response of well chambers relative to the WAFAC has been demonstrated to depend on both the emergent spectrum and emission anisotropy (Mitch *et al* 2002). Note the difference, shown in figure 1, in the well chamber response for both  $^{103}\text{Pd}$  and  $^{125}\text{I}$  seed models that contain silver spheres, which results in a more anisotropic emission pattern than, for example, seeds with an internal silver wire. The anisotropy of emissions in the plane of the source long axis is characterized by mounting the source horizontally and taking x-ray spectrometry measurements at discrete rotation angles about the axis perpendicular to the mid-point of the long axis of the source. The air-anisotropy ratio,  $\alpha_S$ , is calculated using the equation

$$\alpha_S = \frac{S_K^{\text{Spec}}(0) + S_K^{\text{Spec}}(\pi)}{S_K^{\text{Spec}}(\pi/2) + S_K^{\text{Spec}}(3\pi/2)}, \quad (2)$$

where  $S_K^{\text{Spec}}(\theta)$  is the air-kerma strength calculated from the emergent spectrum

$$S_K^{\text{Spec}} = d^2 \sum_i \dot{\Phi}_i \cdot E_i \cdot \left( \frac{\mu_{\text{en}}}{\rho} \right)_i, \quad (3)$$

where  $d$  is the source-to-aperture distance,  $\dot{\Phi}_i$  is the photon fluence rate and  $E_i$  is the energy of the  $i$ th spectral line. The angle  $\theta = 0^\circ$  when the long axis of the source is perpendicular to the face of the HPGe spectrometer. As shown in figure 2, the air-anisotropy ratio has been used to explain variations in well chamber response coefficients observed for sources having the same emergent spectrum on their transverse axis.

In this example, the 2.6% decrease in the response coefficient (figure 2(a)) was caused by an unexpected change in the degree of emission anisotropy due to a manufacturing anomaly. The change in anisotropy was indicated by a 38% decrease in the air-anisotropy ratio (figure 2(b)). Well-ionization chamber response effects due to spectrum differences are able to be separated from those due to source internal structure and self-absorption effects, which influence the anisotropy of x-ray emissions from the source.

**1.1.2. PTB calibrations of  $^{125}\text{I}$  and  $^{103}\text{Pd}$  sources with the Grossvolumen Extrapolationskammer (GROVEX).** To measure the air-kerma rate of LDR brachytherapy seeds, the Physikalisch-Technische Bundesanstalt (PTB) developed the Grossvolumen Extrapolationskammer (GROVEX) (Selbach *et al* 2008). The GROVEX is a cylindrical, parallel plate extrapolation chamber with thin graphite electrodes and a large volume. Air-kerma rate,  $\dot{K}_\delta$ , is determined using the equation

$$\dot{K}_\delta = \left( \frac{\bar{W}}{e} \right) \frac{1}{\rho_{\text{air}} A_{\text{eff}}} \left( \frac{d(kI)}{ds} \right) \prod_i k_i, \quad (4)$$

where  $A_{\text{eff}}$  is the effective area of the collection electrode,  $d(kI)/ds$  is the increment of corrected ionization current per increment of chamber depth and  $k_i$  are correction factors. The brachytherapy source to be calibrated is mounted vertically and is rotated during the measurement to average out equatorial anisotropy. The x-rays pass through a 0.1 mm thick aluminium filter prior to entering the measurement volume, and the front, high-voltage electrode is 30 cm from the seed. The diameter of the back, collection electrode is 10.0 mm, with the distance between the electrodes being adjustable from 0 cm to 20 cm. A comparison performed in 2005 for the calibration of three  $^{125}\text{I}$  and three  $^{103}\text{Pd}$  seeds by NIST, the University of Wisconsin Accredited Dosimetry Calibration Laboratory (UWADCL) and PTB showed agreement to better than 1.5%.

**1.1.3. University of Wisconsin calibrations of  $^{125}\text{I}$ ,  $^{103}\text{Pd}$  and  $^{131}\text{Cs}$  sources with the variable-aperture free-air chamber (VAFAC).** The UWADCL calibration system for low-energy brachytherapy sources is called the variable-aperture free-air chamber (VAFAC) (Culbertson *et al* 2006). The VAFAC is similar in its design to the NIST WAFAC, except that it is operated in an extrapolation mode, can accommodate apertures of various diameters and is sensitive up to an energy of 70 keV. Air-kerma strength,  $S_K$  is calculated using the equation

$$S_K = \left( \frac{\bar{W}}{e} \right) \frac{d^2}{\rho_{\text{air}} A_{\text{eff}}} \left( \frac{d(kI)}{ds} \right) \prod_i k_i, \quad (5)$$

where all quantities have been defined above. The source is held in a vertical position at 30 cm from the chamber's entrance aperture by four thin nylon threads. Two stepper motors rotate the source during the measurement to average out anisotropy. An aluminium filter of 0.086 mm thickness removes titanium x-rays from the beam. A series of five brass apertures with a range of diameters from 5.0 cm to 16.5 cm can be used to study volume-averaging effects. The front and

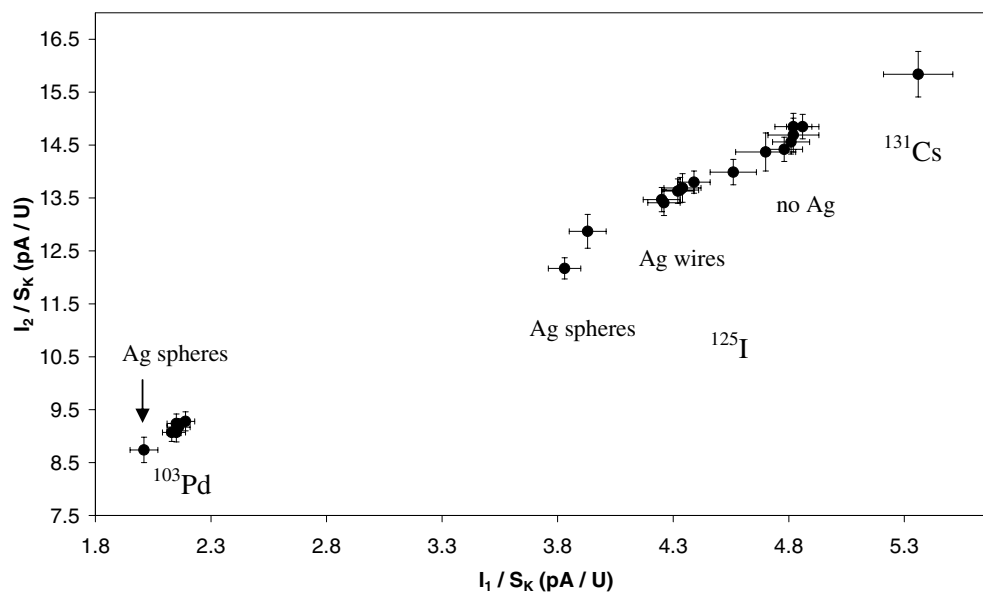


**Figure 1.** Correlation of the response coefficients of two well-ionization chambers for various  $^{103}\text{Pd}$ ,  $^{125}\text{I}$  and  $^{131}\text{Cs}$  source models.

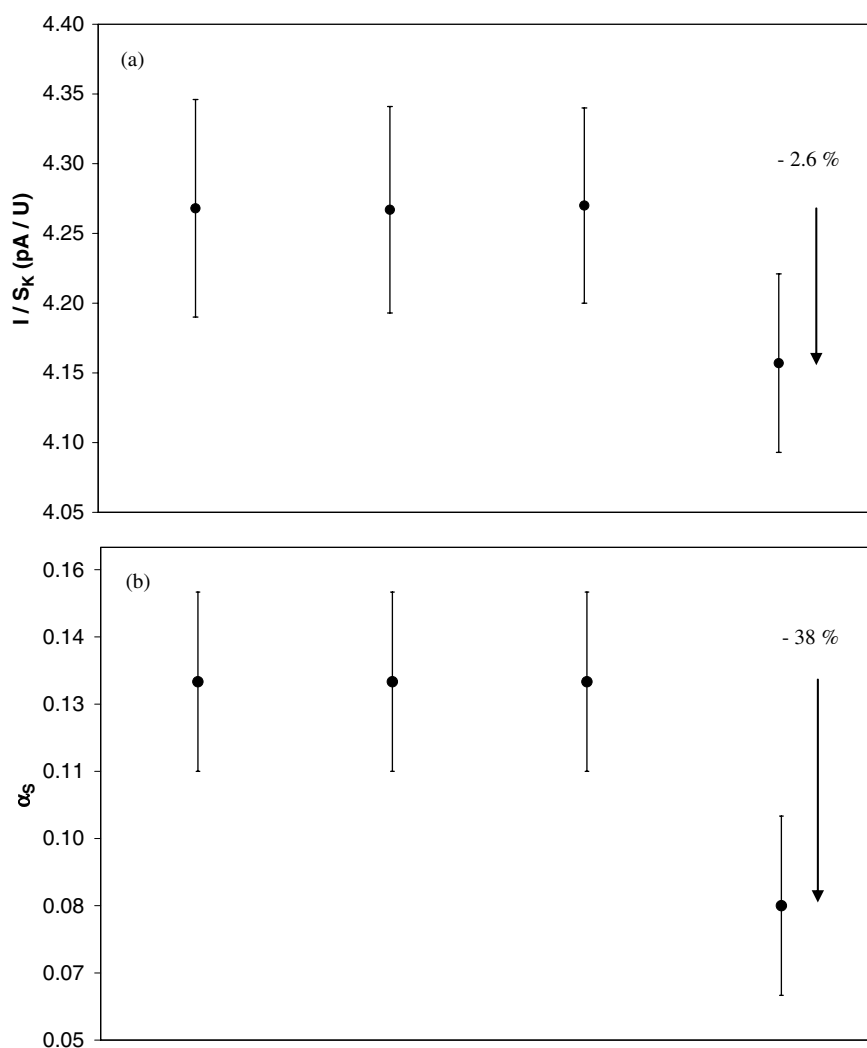


**Figure 2.** (a) Well chamber response coefficients and (b) air-anisotropy ratios for sources of the same model from different batches illustrating the effect of a change in anisotropy. All sources had the same measured emergent spectrum on the transverse axis.

back electrodes consist of graphite diffused onto thin sheets of polyethylene. The diameter of the collection electrode is 40 cm, and the distance between the electrodes is varied from 50 mm to 150 mm in 20 mm increments for a typical measurement series. A comparison with NIST of results from three  $^{125}\text{I}$  and three  $^{103}\text{Pd}$  seeds calibrated on the VAFAC (using the 8 cm aperture) showed agreement within 0.7% of the NIST air-kerma strength values.

**1.1.4. NPL calibrations of  $^{125}\text{I}$  seeds.** The National Physical Laboratory (NPL) provides air-kerma rate calibrations of  $^{125}\text{I}$  seeds using their secondary standard radionuclide calibrator, which is a well-type ionization chamber (Baker *et al* 2002). The calibration coefficient of this chamber is traceable to the NPL primary standard for air-kerma, and the chamber's stability over time is verified by measurement of a  $^{137}\text{Cs}$  source. The primary air-kerma measurement is performed at 1 m from the  $^{125}\text{I}$  seed using a spherical ionization chamber, having a thin, graphite-coated carbon fiber wall, with a volume of 3 L. This chamber is calibrated with the International Organization for Standardization (ISO) 4037 Narrow Spectrum x-ray beams, with the calibration for  $^{125}\text{I}$  being the average of the calibration coefficients at beam energies of 25 keV and 33 keV. As the source is at 1 m from the chamber in air, no aluminium filter is needed to remove the 4.5 keV titanium x-rays from the emergent spectrum. To account for the anisotropy of source emissions, the seed is rotated at  $45^\circ$  intervals about its long axis between measurements, and the mean of the eight measurements is calculated. The expanded uncertainty ( $k = 2$ ) for an air-kerma rate measurement is 5.6%. A comparison of NPL measurements with the NIST-traceable air-kerma strength values on the source manufacturer's certificate for three  $^{125}\text{I}$  seeds indicated agreement with the NIST-traceable values within their uncertainties.

**1.1.5. LNHB torus free-air chamber.** The Laboratoire National Henri Becquerel (LNHB) has designed a novel, circular free-air chamber for future air-kerma calibrations of  $^{125}\text{I}$  and  $^{103}\text{Pd}$  brachytherapy sources. The chamber will be in the shape of a torus with a rectangular cross-section. This design eliminates the need to rotate the source during the measurement to compensate for the anisotropy of emissions about the axis of the source. Also, the chamber has a fixed volume, so there are no moving parts. Other expected advantages of this design include a large signal to noise ratio, a simpler way to specify the source-to-detector distance (which is equal to the inner torus radius), non-critical source positioning, collimator shape conformant with the photon field shape (i.e. very low inverse-square correction) and a low polar averaging angle ( $\pm 2^\circ$ ).

## 1.2. Gamma-ray-emitting LDR brachytherapy sources

**1.2.1. NIST calibration of LDR  $^{192}\text{Ir}$  and  $^{137}\text{Cs}$  sources.** The calibration of high-energy, gamma-ray-emitting brachytherapy sources is performed at NIST using spherical, graphite-walled cavity ionization chambers (Seltzer

and Bergstrom 2003). The exposure,  $X$ , is determined by the equation

$$X = \frac{Q_{\text{air}}}{V\rho_{\text{air}}} \frac{(\bar{S}/\rho)_{\text{graphite}}}{(\bar{S}/\rho)_{\text{air}}} \frac{(\bar{\mu}_{\text{en}}/\rho)_{\text{air}}}{(\bar{\mu}_{\text{en}}/\rho)_{\text{graphite}}} \prod_i k_i, \quad (6)$$

where  $Q_{\text{air}}$  is the collected charge,  $V$  is the volume of the cavity,  $\rho_{\text{air}}$  is the density of air,  $(\bar{S}/\rho)$  is the mean electron-fluence-weighted electron mass stopping power,  $(\bar{\mu}_{\text{en}}/\rho)$  is the mean photon-energy-fluence-weighted mass energy-absorption coefficient and  $k_i$  are correction factors. The air-kerma strength,  $S_K$  is calculated from the exposure rate,  $\dot{X}$ , using the equation

$$S_K = \left( \frac{\bar{W}}{e} \right) \frac{d^2}{(1 - \bar{g})} \dot{X}, \quad (7)$$

where  $g$  is the fraction of the kinetic energy of electrons liberated by photons that is lost in radiative processes (bremsstrahlung) in air.  $\bar{g}$  is the mean value of  $g$  averaged over the distribution of air-kerma with respect to the electron energy.

For  $^{137}\text{Cs}$  sources, measurements of the exposure rate were performed in an open-air geometry to minimize scatter contribution to the measured charge, using a spherical, graphite-walled air-ionization chamber with a volume of about  $1 \text{ cm}^3$  (Loftus 1970). Several 'working standard' sources were calibrated using this method. A large volume (2.8 L) spherical cavity chamber made of an aluminium alloy is used for calibration of brachytherapy sources using a replacement method. That is, a working standard source is placed at about 1 m from the chamber, and the ionization current is measured. Then, the standard source of known air-kerma strength is replaced by the brachytherapy source to be calibrated, and the ionization current from the unknown source is measured. The air-kerma strength of the unknown source is calculated by multiplying the air-kerma strength of the standard source by the ratio of the ionization current from the unknown source to that of the standard source. The expanded uncertainty ( $k = 2$ ) for air-kerma strength calibrations of LDR  $^{137}\text{Cs}$  sources is 2%.

For LDR  $^{192}\text{Ir}$  sources, measurements of the exposure rate were performed in an open-air geometry using a spherical, graphite-walled air-ionization chamber with a volume of about  $50 \text{ cm}^3$  (Loftus 1980). Due to the inadequate signal produced by a single source, arrays of approximately 50 sources were assembled to perform the cavity chamber measurements. The ionization current for each individual seed was then measured using a large volume (3.4 L) spherical-aluminium re-entrant chamber. The calibration coefficient of the re-entrant chamber is the quotient of the exposure rate of the array as measured by the cavity chamber and the sum of the ionization currents from all the seeds in the array. Calibration of individual LDR  $^{192}\text{Ir}$  brachytherapy sources is accomplished using the re-entrant chamber, in conjunction with measurements of the response of the re-entrant chamber to a  $^{226}\text{Ra}$  source to verify its stability over time. The expanded uncertainty ( $k = 2$ ) for air-kerma strength calibrations of LDR  $^{192}\text{Ir}$  sources is 2%.

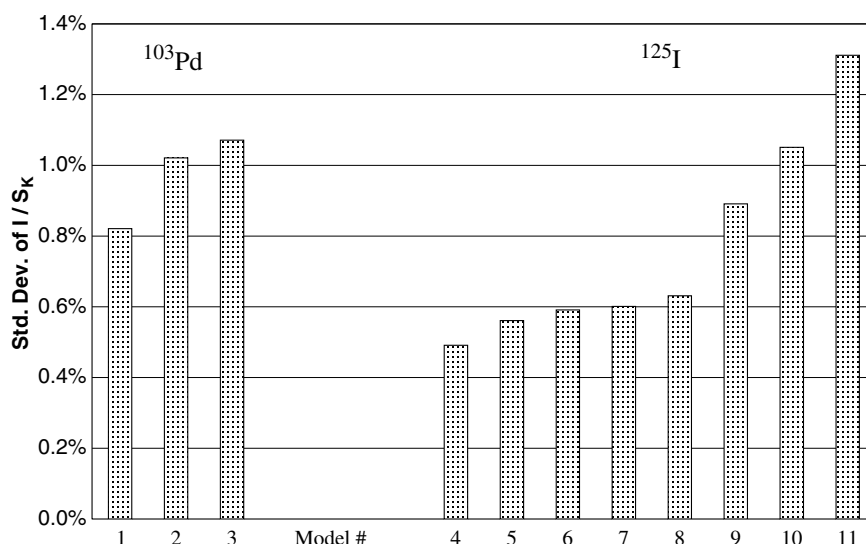


**Figure 3.** Standard deviation of well chamber response coefficient for various  $^{103}\text{Pd}$  (models 1 through 3) and  $^{125}\text{I}$  (models 4 through 11) sources showing the batch-to-batch variability in  $I/S_K$ .

**1.2.2. NPL calibrations of LDR  $^{192}\text{Ir}$  wires and pins.** As for  $^{125}\text{I}$  seeds, NPL provides air-kerma rate calibrations of  $^{192}\text{Ir}$  wires and pins using their secondary standard radionuclide calibrator, which is traceable to the NPL air-kerma primary standard (Rossiter *et al* 1991, Sephton *et al* 1993). The primary air-kerma measurement is performed on a 10 mm length of each source design using the same 3 L chamber described above for  $^{125}\text{I}$  seed calibrations. The chamber is calibrated in x-ray beams of average energies from 33 keV to 250 keV as well as in  $^{137}\text{Cs}$  and  $^{60}\text{Co}$  gamma-ray beams. The calibration coefficient is determined by an appropriate weighting of the energy response of the chamber by the relative contribution to the air-kerma from each line of the source energy spectrum. The expanded uncertainty ( $k = 2$ ) for an  $^{192}\text{Ir}$  air-kerma rate measurement is 1.5%.

## 2. Transfer and maintenance of air-kerma strength standards for LDR brachytherapy

### 2.1. Low-energy x-ray emitting LDR brachytherapy sources

In 2004, the American Association of Physicists in Medicine (AAPM) Calibration Laboratory Accreditation Subcommittee published procedures for the establishment and maintenance of air-kerma strength standards for low-energy photon-emitting brachytherapy sources at the Accredited Dosimetry Calibration Laboratories (ADCLs) (DeWerd *et al* 2004). The initial transfer of the NIST air-kerma strength standard for a particular source model to the ADCLs is accomplished by circulating a batch of three WAFAC-calibrated sources among all ADCLs. Subsequent annual checks involving circulation of an additional three-source batch among NIST and the ADCLs ensures accurate maintenance of the NIST standard. The full suite of characterization measurements described above is employed by NIST not only for the purpose of quality assurance of WAFAC measurements but also to maintain accuracy in the transfer of standards to the ADCLs. Data

from the ADCLs and the source manufacturer, in addition to the results of NIST measurements, are compiled and checked as a function of time to ensure the continuous validity of the calibration traceability chain from NIST to ADCLs and manufacturers. After over five years of experience with source calibration and characterization, it is apparent from figure 3 that the magnitude of the effects of source-to-source and batch-to-batch variations on achievable tolerance levels for secondary standards based on well chambers is source-model dependent.

### 2.2. Gamma-ray-emitting LDR brachytherapy sources

For LDR, high-energy gamma-ray-emitting brachytherapy sources containing the radionuclide  $^{192}\text{Ir}$  or  $^{137}\text{Cs}$ , the initial transfer of the NIST air-kerma strength standard for a particular source model to the ADCLs was first accomplished many years ago. Periodic measurement quality assurance (MQA) tests to ensure accurate maintenance of standards at the ADCLs have taken place. The procedure for maintenance of the NIST standard by source manufacturers was published by the AAPM high-energy brachytherapy dosimetry (HEBD) subcommittee in 2007 (Li *et al* 2007). It is recommended that annual calibration checks on sources or equipment be performed by either NIST or an AAPM-accredited ADCL.

## 3. Air-kerma standards for high dose rate (HDR) brachytherapy sources

### 3.1. Introduction

**3.1.1. Brachytherapy sources and afterloaders.** HDR brachytherapy is an interesting alternative to external beam radiotherapy for the treatment of some cancers. The radioactive material is implanted temporarily into the tumor by a remote controlled afterloading unit. HDR brachytherapy has considerable importance in North America (more than 1000 units in operation). In Europe, even though its development has increased during the last years, the number of HDR units



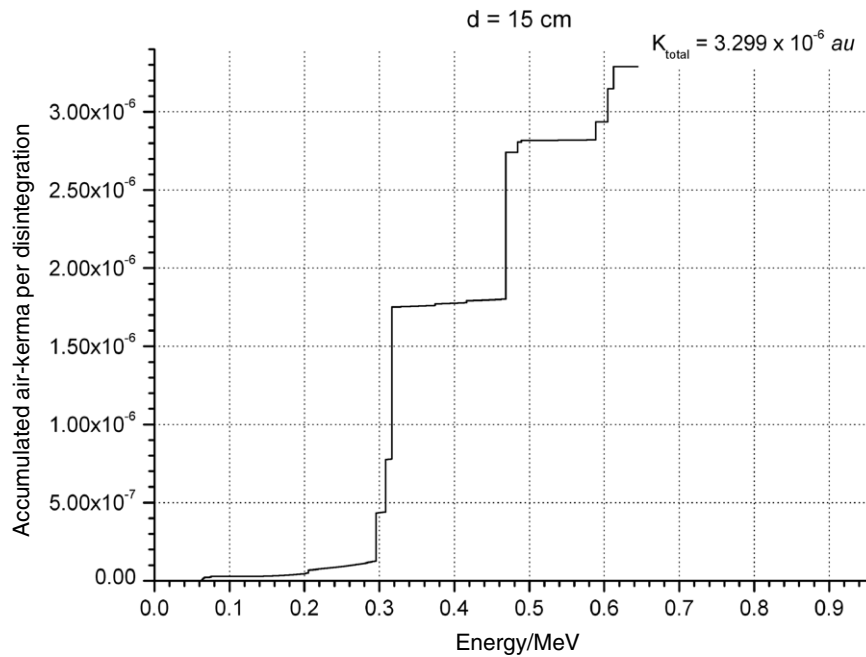


**Figure 4.** Monte Carlo determination of the accumulated air-kerma as a function of photon energy (source: Nucletron microSelectron V2, medium: vacuum).

is still less than half that of North America. In some countries, pulsed dose rate (PDR) brachytherapy is also employed (about 40 units in operation in France). It is very similar to HDR except that the source activity is 10 to 20 times lower.

Treatment times in HDR brachytherapy are in the minute range and typical dose rates at 1 cm are larger than  $12 \text{ Gy h}^{-1}$ .  $^{192}\text{Ir}$  is the most common isotope ( $^{60}\text{Co}$  is also used to a much lesser extent).  $^{192}\text{Ir}$  is obtained by neutron activation of natural iridium. Because of its high specific activity,  $^{192}\text{Ir}$  sources can be miniaturized. Nucletron, Varian and Gammamed (today a subsidiary of the Varian Company) are the major manufacturers of HDR afterloaders. (In this paper certain commercially available products are mentioned by name. These identifications are for informational purposes only. They do not imply that they are the best or only instruments available, nor do they imply any endorsement by NIST or LNHB.) The sources comprise a  $^{192}\text{Ir}$  cylinder ( $L = 3.5 \text{ mm}$  to  $10.0 \text{ mm}$ ,  $\varnothing 0.35 \text{ mm}$  to  $0.65 \text{ mm}$ ) surrounded by a metallic encapsulation (stainless steel, titanium alloy)  $100 \mu\text{m}$  to  $200 \mu\text{m}$  thick (see ESTRO (2004)). The active part is welded to a stainless steel cable of typical length  $1500 \text{ mm}$ .

The decay of  $^{192}\text{Ir}$  is relatively fast ( $T_{1/2} = 73.827(13) \text{ d}$ , i.e. 1% decay per day) (see DDEP (2004)), so the sources are usually replaced quarterly in hospitals.

**3.1.2. Definitions.** HDR brachytherapy sources are calibrated in air in terms of air-kerma strength (symbol:  $S_K$  (Nath *et al* 1995)) in North America and reference air-kerma rate (RAKR) in Europe (symbol:  $\dot{K}_R$  (ICRU 1985, 1997)):

$$\begin{aligned} S_K &= \dot{K}(d) \times d^2, \\ \dot{K}_R &= \dot{K}(d) \times \left( \frac{d}{d_{\text{ref}}} \right)^2, \end{aligned} \quad (8)$$

where  $\dot{K}(d)$  denotes the air-kerma rate measured at distance  $d$  along the transverse bisector of the source and  $d_{\text{ref}}$  is the reference distance. Since  $d_{\text{ref}} = 1 \text{ m}$ , the two quantities are equivalent. They are defined for a point volume of air placed into an infinite volume of vacuum (i.e. no beam attenuation, no scattering).

### 3.2. Methods for dosimetric standard realization

**3.2.1.  $^{192}\text{Ir}$  radioactive decay.**  $^{192}\text{Ir}$  decays by  $\beta$ -emission to  $^{192}\text{Pt}$  (95%) and by electron capture to  $^{192}\text{Os}$  (5%). Electrons are essentially stopped in the source encapsulation, therefore HDR sources can be considered as  $\gamma$  emitters. Bremsstrahlung photons arising from the  $\beta$ -decay contribute only by 0.2% to 0.3% to the total air-kerma (Borg and Rogers 1999) therefore they can be neglected as a first approximation. The emission spectrum is relatively complex with about 35 lines extending from fluorescence x-rays up to  $1.378 \text{ MeV}$  (DDEP 2004). As shown in figure 4, about 96% of the total air-kerma is attributed to photons of energies larger than  $295 \text{ keV}$ . The air-kerma-weighted average energy is  $398.6 \text{ keV}$ .

The most common radiochemical impurity is  $^{194}\text{Ir}$  ( $\beta$  average energy  $345 \text{ keV}$ ). This isotope is inevitably produced during activation of  $^{193}\text{Ir}$  (natural abundance 63%). However, due to its fast decay ( $T_{1/2} = 19.3(1) \text{ h}$ ), this isotope virtually disappears within one week after activation.

### 3.2.2. Indirect methods for dosimetric standard realization.

**3.2.2.1. Principle.** The technique was originally developed by Goetsch *et al* in the 1990s for  $^{192}\text{Ir}$  (Goetsch *et al* 1991). Since the average energy of  $^{192}\text{Ir}$  lies approximately halfway between average energies of NIST M250 technique x-rays and  $^{137}\text{Cs}$  gamma rays, a therapy level cavity ionization chamber

is calibrated in air in these reference beams, and its calibration coefficient  $N_K(\text{Ir})$  for the  $^{192}\text{Ir}$  spectrum is obtained by linear interpolation. Then,  $\dot{K}_R$  is obtained using the following equation:

$$\dot{K}_R = N_K(\text{Ir}) \cdot I \cdot \prod_i k_i \cdot \left(\frac{d}{d_{\text{ref}}}\right)^2, \quad (9)$$

where  $I$  denotes the ionization current (corrected for atmospheric effects, leakage and radioactive decay),  $k_i$  are correction factors (described below) and  $d$  is the source-to-detector distance.

The ionization chamber has to be chosen among those that show the lowest energy dependence of response and the best long term stability. The NE2571 Farmer ionization chamber for instance combines the two advantages: the variation of its calibration coefficient from M250 x-rays to  $^{60}\text{Co}$  is lower than 0.9% and it has proven long term stability (drift <0.1% over 4 years). For all calibrations it must be fitted with the build-up cap corresponding to the most energetic beam. Originally, in the Goetsch paper the interpolated  $N_K(\text{Ir})$  was obtained in the following way:

$$A_w N_K(^{192}\text{Ir}) = \frac{1}{2} [A_w N_K(250 \text{ kV}) + A_w N_K(^{137}\text{Cs})], \quad (10)$$

where  $N_K(i)$  stands for the calibration coefficient in beam ( $i$ ) and  $A_w$  denotes the wall correction factor. This approach has been recommended by IAEA (1999, 2002) and followed by several laboratories such as LNHB in France. Recently Mainegra-Hing and Rogers (2006) pointed out that this method is flawed. First, the averaging should be based on  $1/N_K$  values instead of  $N_K$ , and secondly that no wall correction factors  $A_w$  are needed. Thus the interpolated  $N_K$  is simply given by

$$\frac{1}{N_K(^{192}\text{Ir})} = \frac{1}{2} \times \left[ \frac{1}{N_K(250 \text{ kV})} + \frac{1}{N_K(^{137}\text{Cs})} \right]. \quad (11)$$

Hopefully, since ionization chambers are chosen for their low energy sensitivity, the error introduced using the flawed method is usually very small. For instance, the total change in the LNHB determination of  $N_K(\text{Ir})$  is on the order of 0.02%.

A more detailed interpolation technique has been developed by some national laboratories (Verhaegen *et al* 1992, Van Dijk 2003). In addition to  $^{137}\text{Cs}$  and  $^{60}\text{Co}$ , the ionization chamber is calibrated in a large range of narrow spectra x-ray beams (typically 8 to 25 beams from 10 kV to 300 kV). The chamber calibration coefficient for the  $^{192}\text{Ir}$  spectrum is obtained by weighting the individual calibration coefficients with respect to the peak heights in the  $^{192}\text{Ir}$  spectrum. This leads in principle to a better interpolated value of  $N_K(\text{Ir})$ . However, as pointed out by Mainegra-Hing and Rogers (2006), the linear interpolation between the highest energetic x-rays (300 kVp) and  $^{137}\text{Cs}$  is still needed, all the more because the largest part of the air-kerma comes from photons of energies larger than 300 keV (see section 3.2.1).

**3.2.2.2. Source-to-detector distance measurement.** RAKR determination involves the measurement of the source-to-detector distance. This length is typically on the order

of 100 mm for small volume chambers. Therefore, this measurement is critical: a  $\pm 0.5$  mm distance error would lead to a  $\pm 1\%$  error in the RAKR determination. However, no mechanical means have been adapted for this measurement due to the lack of a rigid surface where the instrument can be fixed. There is no evidence that the required precision level is influenced by the chamber effective centre not being located at its geometrical centre.

At LNHB a non-contact, indirect distance measuring method has been developed. The ionization chamber is rotated around the source on a precisely known radius and the source-to-detector distance is derived from the current versus angle curve (see Douysset *et al* (2005)). As shown in figure 5, the chamber is attached to a combination of remote controlled rotation and translation stages, which allow one to set the radius of the rotation in the range from 0 mm to 225 mm. This technique is extremely sensitive and its accuracy has been estimated to be  $\pm 52 \mu\text{m}$ , taking into account all known geometrical defects. Another advantage of this method is that the actual centre of radioactivity is determined; any source emission equatorial anisotropy is automatically accounted for.

**3.2.2.3. Correction factors.** Several correction factors have to be taken into account. The first one ( $k_{\text{att}}$ ) corrects for beam attenuation between the source and the detector. This attenuation is due to air and to the source catheter (a polystyrene tube with wall thickness of 2 mm is used at LNHB). The correction is obtained by Monte Carlo simulation. Source spectra are estimated for two configurations: source alone placed into vacuum and the full experimental set-up (source, catheter, holders and air).  $k_{\text{att}}$  is the ratio of the air-kerma rates obtained in the two different configurations. To a great extent, the beam attenuation is compensated by scattering. In the range from 100 mm to 200 mm,  $k_{\text{att}}$  is constant and equal to 1.0038 (13). Selvam *et al* (2001) concluded in a separate Monte Carlo study that air attenuation was exactly cancelled by air scattering.

Due to high dose gradient around the brachytherapy sources and to the size of ionization chambers, there is a strong fluence variation over the detector surface. This yields to non-uniform electron fluence in the active volume.  $k_N$  corrects for this effect. It is obtained from theoretical works of Kondo and Randolph (1960) and Bielajew (1990). This correction depends on chamber geometry and source-to-detector distance. For the NE2571 chamber,  $k_N$  is as high as 1.010 at 100 mm. Much lower corrections can be obtained with spherical ionization chambers.

RAKR is defined in the absence of scattered radiations. Even though experimental set-ups are designed to minimize scattering (low atomic number ( $Z$ ) materials for supports, and chamber and source at least 1 m away from scattering surfaces), the scattering contribution might not be negligible (up to 5% of the measured signal at 200 mm according to Stump *et al* (2002)). One way to measure the current fraction due to scattering ( $I_{\text{scatt}}$ ), is to use the multiple distance method: the current is measured for different source-to-detector distances and discrepancies from the inverse-square law are attributed to scattering.  $I_{\text{scatt}}$  is determined redundantly using typically 8

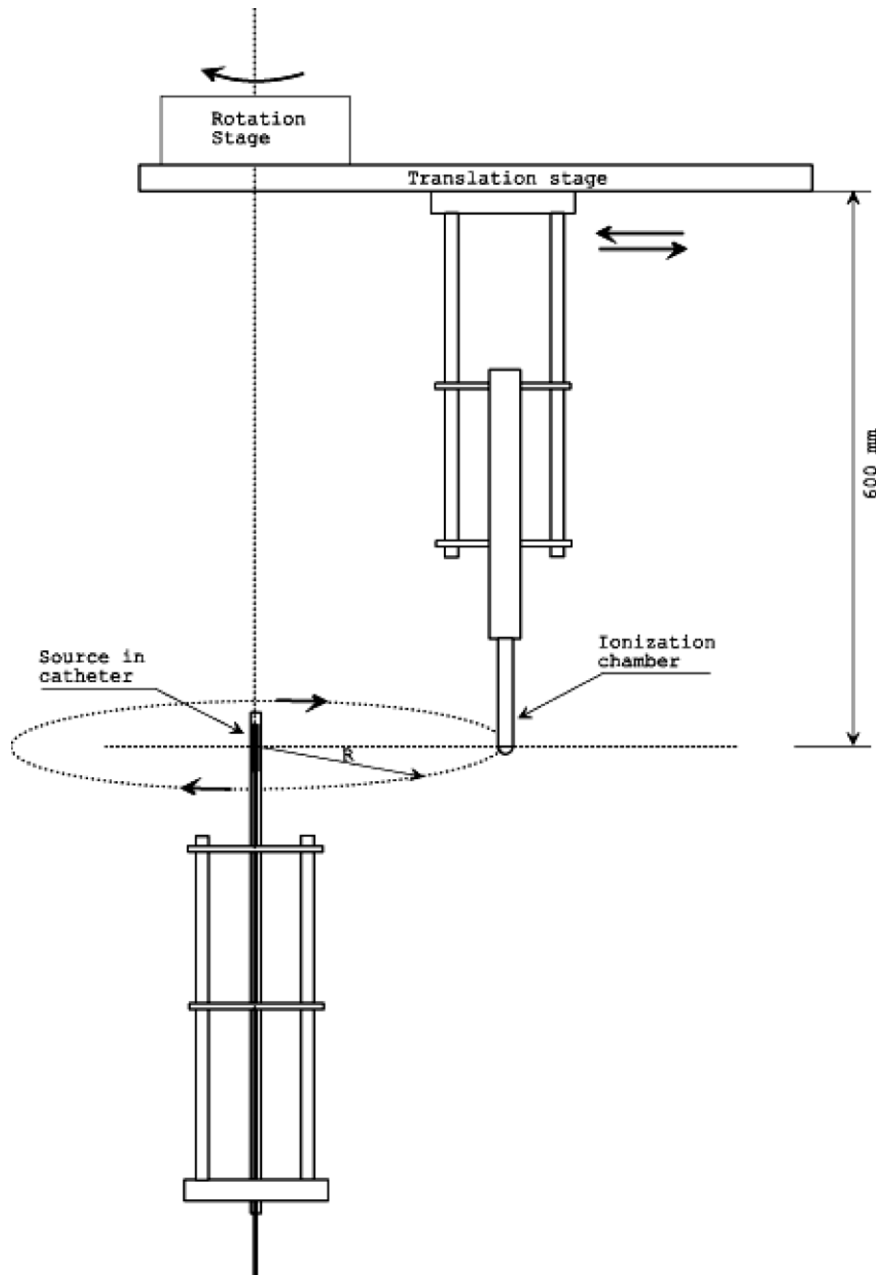


**Figure 5.** Overview of the LNHB experimental set-up for the measurement of  $^{192}\text{Ir}$  RAKR (not to scale).

to 10 distances. Assuming  $I_{\text{scatt}}$  is independent of the distance (which has been proven to be true over distances from 10 cm to 40 cm, see Goetsch *et al* (1991))  $I_{\text{scatt}}$  can be determined by

$$I_{\text{meas}}(d) - I_{\text{back}} = I_{\text{scatt}} + \frac{\alpha}{d^2} \times \frac{1}{k_{\text{N}}(d) \times k_{\text{att}}(d)}, \quad (12)$$

where  $I_{\text{meas}}$  and  $I_{\text{back}}$  represent the measured signal and the background current (measured without any radioactive source), respectively,  $\alpha$  is a constant,  $d$  is the source-to-detector distance,  $k_{\text{N}}(d)$  is the non-uniformity correction factor and  $k_{\text{att}}$  is the attenuation correction. Typically for the LNHB set-up,  $I_{\text{scatt}}$  represents about 1% of the signal measured at 200 mm.

Another technique has been developed at UWADCL to determine both the actual source-to-detector distance and the scattered current in a single step. The source-to-detector

distance is determined approximately, and the multiple distance technique is applied introducing one extra free parameter in equation (12) (Stump *et al* 2002). Namely,  $d$  is replaced by  $(d + c)$  where  $c$  denotes the distance correction term. This results in a slightly larger uncertainty but its implementation is fairly simple.

Scattering can also be minimized by collimating the  $^{192}\text{Ir}$  photon beam. The source is loaded into a lead housing fitted with a collimator to produce a circular beam. This technique is used at PTB. In this configuration the scattered fraction can be determined by the shadow shield method (see for instance Verhaegen *et al* (1992)). The direct beam is stopped by a cone-shaped shield placed between the source and the detector. The current fraction due to scattering is equal to the residual detected signal. It should also be mentioned that PTB has been



very active in developing methods for determining RAKR for the past 15 years (Büermann *et al* 1995) and has developed a very sophisticated and precise calibration facility (Selbach and Büermann 2004, Selbach 2006).

**3.2.2.4. Practical considerations.** At LNHB the  $^{192}\text{Ir}$  HDR sources are replaced annually, and each time the RAKR is determined using the above mentioned method. The total uncertainty of the source calibration is 1.2% ( $k = 2$ ). As a constancy check, laboratory transfer dosimeters are also calibrated before and after each source calibration. The maximum accepted deviation for their calibration coefficients is  $\pm 0.3\%$ .

Two calibration campaigns are organized for medical physicists' instruments. The first one occurs immediately after the source calibration and lasts for three months, and the second one starts after eight months of source decay. This allows us to perform calibrations in a PDR-like mode. Even though the HDR and PDR source designs are slightly different, this offers to PDR brachytherapy users the opportunity to get a calibration coefficient for conditions as similar as possible to their operating conditions. The expanded uncertainty for well-type chamber calibration at LNHB is 1.3%.

**3.2.3. Direct methods for dosimetric standard realization.** For a long time, the set-up of a direct primary method for the realization of an air-kerma standard for  $^{192}\text{Ir}$  has been hampered by the fact that the average emission energy was too high for free-air chambers and too low for the validity of the Bragg–Gray theory. Recently, Monte Carlo codes became powerful enough to predict the necessary correction factors (see Borg *et al* (2000)). In the last decade, NPL has started the development of such a standard (Sander and Nutbrown 2006). It is based on a volume-calibrated graphite spherical ionization chamber. The source is located 1.433 m away from the detector in a lead housing fitted with a collimator. Deviations from Bragg–Gray conditions are accounted for by applying a Monte Carlo estimated electron fluence correction factor. Currently the total uncertainty of the source calibration is 0.8% ( $k = 2$ ).

## 4. Transfer and maintenance of HDR air-kerma standards

### 4.1. Introduction

End user control of source air-kerma rate is recognized by the medical physics community to be an essential step of the MQA process (Kutcher *et al* 1994, Nath *et al* 1997). The HDR brachytherapy sources are provided by manufacturers together with a source certificate stating the RAKR (or AKS) with an uncertainty of  $\pm 5\%$  ( $k = 3$ ). Using this value for treatments without any check by the medical physicist could be dangerous to the patient. Indeed at least two error risks are identified. First the source might have been measured too early after fabrication (i.e. while still contaminated with  $^{194}\text{Ir}$ ) or, even worse, there is a risk that the source certificate might not be the one for the source actually received (because of their very small dimensions the sources are not easily identified).

### 4.2. Well-type ionization chambers

**4.2.1. Characteristics.** Well-type ionization chambers are ideally suited for routine calibrations of brachytherapy sources (Goetsch *et al* 1992). Due to the nearly  $4\pi$  geometry and the large detection volume, the ionization current is high and easy to measure with precision. There is also no need of accurate source-to-detector distance measurement and the long term stability can be on the order of  $\pm 0.1\%$  over a period of several years.

The three major manufacturers that are providing brachytherapy well-type chambers are PTW, Standard Imaging and Sun Nuclear Corporation. Collection volumes extend from  $200\text{ cm}^3$  to  $1200\text{ cm}^3$  and typical currents are in the range  $10^{-9}\text{ A}$  to  $10^{-7}\text{ A}$  for HDR sources.

**4.2.2. Precautions for use.** Well-type ionization chambers are very sensitive; therefore it is of primary importance to avoid the detection of scattered photons. It has been shown that the detector when placed close to a wall might overestimate the current by as much as 1% (Podgorsak *et al* 1992). Ideally the detector should be placed at least 1 m away from any scattering surface (wall, floor or ceiling).

The point of maximum response of the detector (often called the 'sweet spot') has to be determined by stepping the source along the well height as shown in figure 6. The response variation has been optimized by manufacturers; usually it varies by less than  $\pm 0.2\%$  over a  $\pm 5\text{ mm}$  displacement around the sweet spot.

Some detectors experience a relatively large high voltage polarity sensitivity (up to 0.4% difference). This is not a major drawback when the detector is used at constant polarity. The ion collection efficiency ( $A_{\text{ion}}$ ) of well-type chambers is large, typically  $>99.7\%$ . Volume recombination can be estimated by measurements at two different biases ( $V_1$  and  $V_2$ ) (Boag 1987):

$$A_{\text{ion}} = \frac{1}{k_{\text{ion}}} = \frac{(V_1/V_2)^2 - (I_1/I_2)}{(V_1/V_2)^2 - 1}, \quad (13)$$

where  $I_i$  represents the current measured for voltage  $V_i$ . In the case where  $V_1 = 2 \times V_2$ , it simplifies to (Attix 1984)

$$A_{\text{ion}} = \frac{1}{k_{\text{ion}}} = \frac{4}{3} - \frac{I_1}{3 \times I_2}. \quad (14)$$

Since  $A_{\text{ion}}$  decreases as source activity increases, it is sensible (especially for pressurized chambers) to measure it and to correct the signal to 100% collection efficiency.

Most of the well-type ionization chambers are vented to the atmosphere and therefore the measured signals have to be corrected for air density variations. Reference conditions are  $p_0 = 101.315\text{ kPa}$ ,  $T_0 = 293.15\text{ K}$  (295.15 K in North America). Because of their large size, thermal inertia of well-type chambers is important. Using a miniature thermistor inserted directly into the active volume through the venting hole, it has been shown that several hours might be necessary for the inner temperature to equilibrate with the ambient temperature. No humidity correction is applied. However it has been shown (for at least one type of detector) that

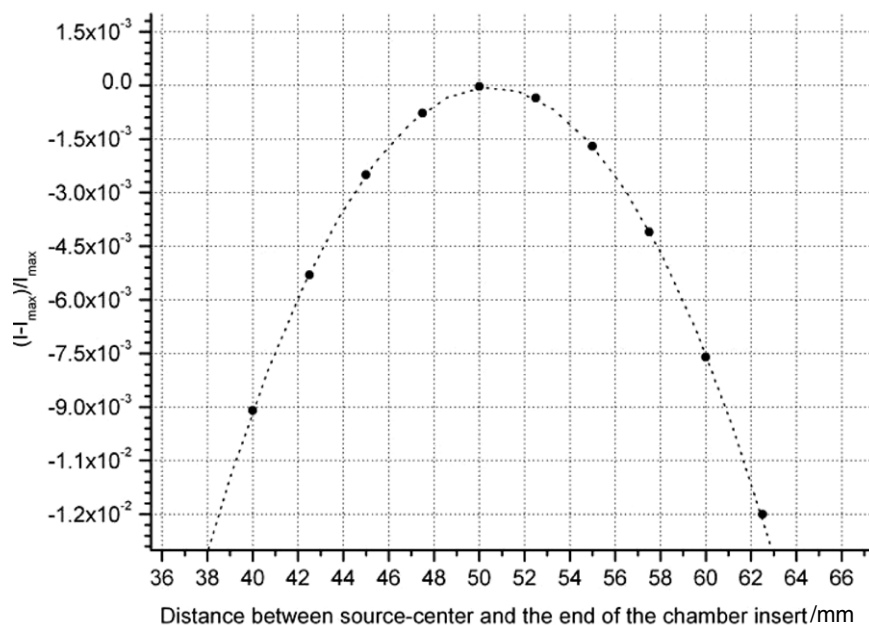


**Figure 6.** Axial response of a Nucletron 077.091 well-type ionization chamber.

the measured signal depended on the surrounding humidity. Up to  $\pm 0.35\%$  signal variation was observed over the annual humidity range (see Poirier and Douysset (2006)). If no correction is applied, it is important to ensure that the humidity remains relatively constant over the course of time.

Usually national dosimetric standards for HDR brachytherapy are based on one single source type. It is therefore questionable if calibration coefficients are directly transferable to another source type (Kutcher *et al* 1994). The active source length and encapsulation thickness are the major differences between the different source types. The average emission energy of  $^{192}\text{Ir}$  is relatively high (close to 400 keV), but since iridium presents the highest density of elements in the periodic table ( $\rho = 22.4 \text{ g cm}^{-3}$ ), the self absorption of photons along the source longitudinal axis is significant. Thus the photon fluence is a function of the polar angle relative to the transverse plane. As required by the RAKR definition, anisotropy is not taken into account during source calibration, with the averaging angles in all cases being lower than  $\pm 5^\circ$ . However, when using a well-type ionization chamber the averaging angles increase up to  $\pm 80^\circ$ . Therefore, possible differences in emission anisotropy from one source type to another are only taken into account while using well-type chambers. Strictly speaking calibration coefficients obtained for one source type are not transferable to another source type. Hopefully, differences in emission anisotropy are mitigated by the inverse-square law. It has been shown experimentally by Stump *et al* (2002) for a set of sources that the calibration coefficients are equivalent to within less than 1%. Recently, a preliminary Monte Carlo study started at LNHB including four different source designs and two models of well-type chambers confirmed this finding. For future work it would be valuable to establish a correction matrix able to convert calibration coefficients between any combination of source design and ionization chamber type.

One Nucletron 077.091 and one Standard Imaging HDR1000+ well-type ionization chamber are used at LNHB as constancy check instruments. They are associated with a medical type electrometer (Standard Imaging MAX4000), on which the ampere and coulomb scales are periodically calibrated, during the source lifetime and after each source replacement. The four year history (see figure 7) shows that the calibration coefficient of the HDR1000+ chamber remained constant within  $\pm 0.1\%$  (using six different sources). For the other system, an unexpected decrease in the calibration coefficient as source activity is decreasing has been detected. As shown in figure 8, the magnitude of the variation is as large as 0.7% between HDR and PDR-like air-kerma rates (see Douysset *et al* (2008a)). This emphasizes the fact that well-type chambers have to be calibrated at the dose rates typically used for the application.

Pressurized well-type chambers are sometimes used. There are two advantages to using this kind of instrument: gas type and pressure can be optimized to improve the ionization current, and there is also no need for pressure and temperature corrections. However, these advantages are partly cancelled by a possible loss of sensitivity of the chamber over time due to gas leakage, which can be as high as 1% per year. This implies a shorter calibration interval and/or periodic constancy checks to maintain the measurement accuracy of these systems.

#### 4.3. Comparison of dosimetric standards

**4.3.1. LNHB/UWADCL bilateral comparison.** In order to validate the French dosimetric standard for HDR brachytherapy, a bilateral comparison was organized in 2004 with UWADCL (Douysset *et al* 2005). Both laboratories were basically using the same measurement method. Since national standards for  $^{137}\text{Cs}$  and  $^{60}\text{Co}$  were changed in the US in 2003 (Seltzer and Bergstrom 2003), it was interesting to measure

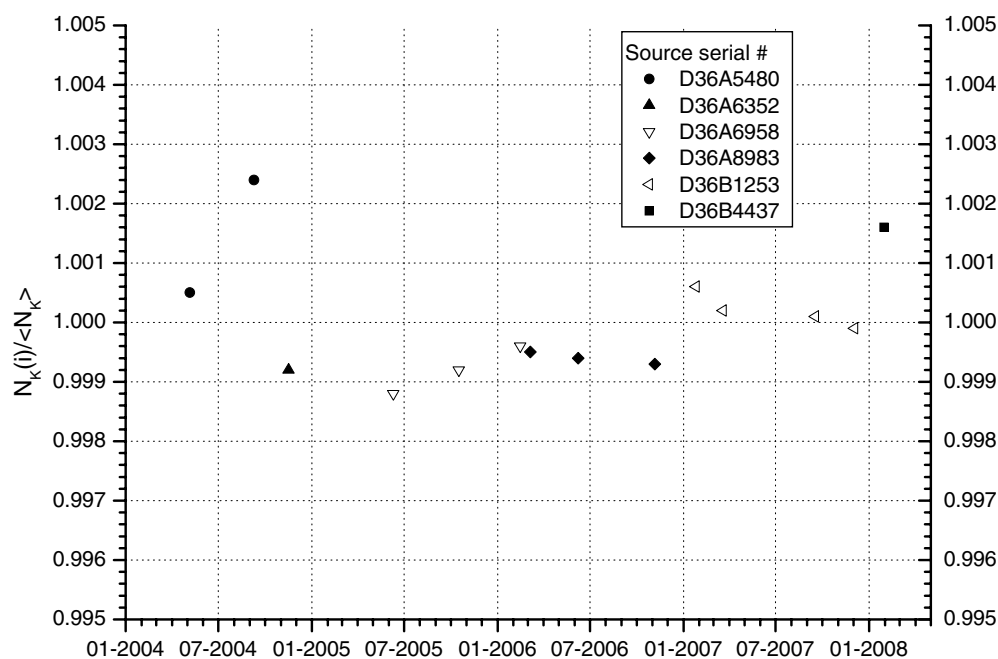


**Figure 7.** Calibration history of the LNHB HDR1000+ well-type ionization chamber. The calibration coefficients were determined for six different sources between 2004 and 2008 and normalized to the running mean.

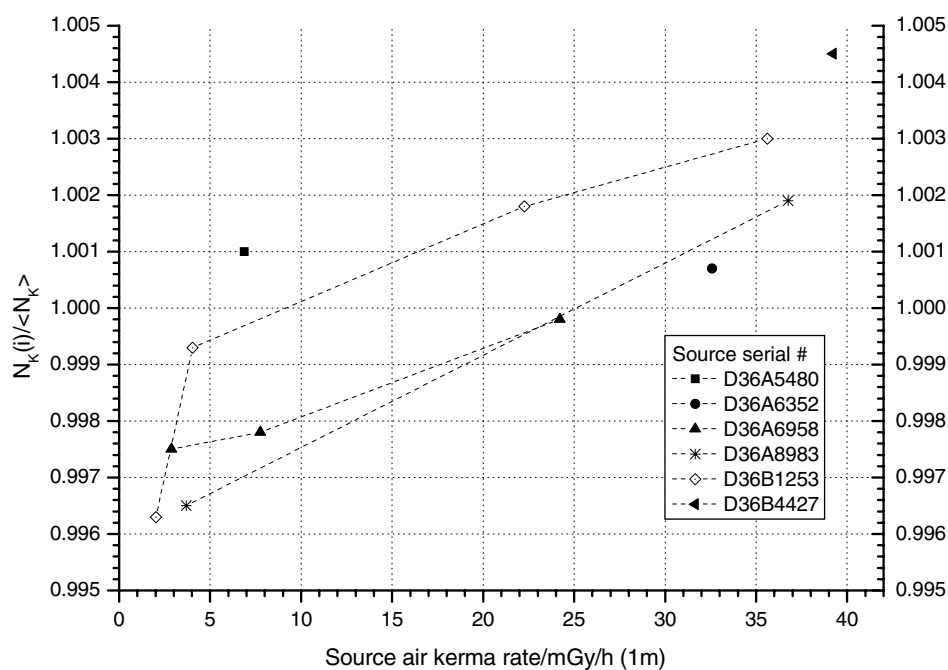


**Figure 8.** Calibration history of the LNHB Nucletron 077.091 well-type ionization chamber as a function of source RAKR. The calibration coefficients were determined for six different sources between 2004 and 2008 and normalized to the running mean.

how these changes affected the  $^{192}\text{Ir}$  standard. The source-to-detector distances were measured using different techniques and the source types were significantly different (Varian Varisource VS2000 and Nucletron microSelectron V2).

A set of three different well-type chambers were calibrated in both laboratories and the calibration coefficients were compared. An excellent agreement relative to calibration standard uncertainties (0.65% and 1.32% for LNHB and UWADCL, respectively) was obtained; discrepancies

ranged between +0.12% and +0.28% (the LNHB calibration coefficients being larger than those determined by UWADCL).

**4.3.2. LNHB/NPL bilateral comparison.** Some years ago NPL started the development of an HDR dosimetric standard. As mentioned above, it is based on a direct method: the source is calibrated with a primary cavity ionization chamber. A LNHB/NPL bilateral comparison was coordinated by the EUROMET organization and was recorded by the BIPM as

a supplementary comparison (EUROMET.RI(I)-S6). Again a set of four well-type ionization chambers and associated medical type electrometers were calibrated in both institutions (see Douysset *et al* 2008b). The two source types used were very similar (Nucletron microSelectron V1 and V2). The results showed that the reported calibration coefficients agreed within +0.47% to +0.63%, which was within the overall standard uncertainties of 0.65% reported by the two laboratories (the LNHb calibration coefficients being larger than those determined by NPL). Following this comparison, NPL revised its primary standard because of a re-evaluation of some correction factors. After this change, the discrepancy range between the two standards was reduced to +0.30% to +0.46%. Even though the methods for the definition of the standards are completely different, an excellent agreement was found for transfer instrument calibrations.

Thus, at this time, the American, English and French dosimetric standards are in agreement within 0.3%, which is essential for clinical applications.

## 5. Dosimetry protocols and data sets for LDR and HDR brachytherapy sources

### 5.1. AAPM TG-43 protocol

In 1988, the Radiation Therapy Committee of the American Association of Physicists in Medicine (AAPM) formed Task Group No. 43 (TG-43) for the purposes of developing a formalism for calculation of dose around interstitial brachytherapy sources and recommending consensus dosimetry data sets for various source models (Nath *et al* 1995). The TG-43 report, published in 1995, contained descriptions of, and dosimetry data for, photon-emitting brachytherapy sources employing  $^{192}\text{Ir}$ ,  $^{125}\text{I}$  or  $^{103}\text{Pd}$  as the encapsulated radionuclide. These sources were all cylindrically symmetric, and contained various materials that functioned as substrates for the deposition of radioactive material during source fabrication and/or radiopaque (high- $Z$ ) markers to facilitate identification in post-implant radiographs. The emergent photon fluence was therefore spatially anisotropic, necessitating a departure from previous methods for calculating dose in media which were based on a point-source geometry.

In the years following publication of the original TG-43 report, the clinical use of low-energy photon-emitting  $^{125}\text{I}$  and  $^{103}\text{Pd}$  brachytherapy sources increased substantially. Numerous companies began to manufacture new seed models, and there was a need to update the TG-43 report. The AAPM Low-energy Interstitial Brachytherapy Dosimetry subcommittee (LIBD) published an update of the original TG-43 report in 2004 (TG-43U1) (Rivard *et al* 2004a, 2004b). In addition to updating the dosimetry data sets for the two  $^{125}\text{I}$  and one  $^{103}\text{Pd}$  seed models addressed by the original TG-43 report, data sets were presented for five additional seed designs. The dose calculation protocol was revised, including a modified definition of air-kerma strength, consistent with a new primary standard developed by NIST which was implemented in 1999.

The continued demand for low-energy brachytherapy sources led to the development of additional new source models

in recent years. In 2007, a supplement to the TG-43U1 report was published, designated TG-43U1S1 (Rivard *et al* 2007). In this report, consensus dosimetry data sets of eight additional sources were published, along with recommendations for applying interpolation and extrapolation techniques to the data sets. The low-energy brachytherapy dosimetry (LEBD) working group continues this effort, and is currently in the process of critically evaluating dosimetry data for the second supplement to the TG-43U1 report.

According to the TG-43U1 protocol, the equation for calculating the two-dimensional dose rate distribution in water  $\dot{D}(r, \theta)$  from a photon-emitting, cylindrically symmetric brachytherapy source is

$$\dot{D}(r, \theta) = S_K \cdot \Lambda \cdot \frac{G_L(r, \theta)}{G_L(r_0, \theta_0)} \cdot g_L(r) \cdot F(r, \theta), \quad (15)$$

where  $r$  is the distance from the centre of the source and  $\theta$  is the polar angle (relative to the source longitudinal axis) to the calculation point. The reference point is located along the transverse axis of the source at  $r_0 = 1 \text{ cm}$  and  $\theta_0 = \pi/2$ . The dose rate is typically expressed in units of  $\text{cGy h}^{-1}$ .  $S_K$  is the air-kerma strength of the source, as realized by the NIST WAFAC (Seltzer *et al* 2003).  $\Lambda$  is the dose rate constant, defined as the ratio of the dose rate in water at the reference point,  $\dot{D}(r_0, \theta_0)$ , to  $S_K$ . The geometry function,  $G_X(r, \theta)$ , accounts for the inverse-square law, neglecting scattering and attenuation by the medium, and is calculated based on either a point- or line-source model of the spatial distribution of radioactive material inside the source capsule. For the point-source approximation,  $G_P(r, \theta) = r^{-2}$ , and for the line-source approximation,  $G_L(r, \theta) = \beta / (Lr \sin \theta)$ , except if  $\theta = 0$ , in which case  $G_L(r, 0) = (r^2 - L^2/4)^{-1}$ .  $\beta$  is the angle subtended by the ends of the line source of length  $L$  with respect to the calculation point. The value of  $L$  is determined by considering the actual internal geometry of source components, and its calculation is described in detail in TG-43U1. The radial dose function,  $g_X(r)$ , quantifies the dose fall-off along the transverse axis of the source due to scattering and attenuation by the medium:

$$g_X(r) = \frac{\dot{D}(r, \theta_0)}{\dot{D}(r_0, \theta_0)} \frac{G_X(r_0, \theta_0)}{G_X(r, \theta_0)}. \quad (16)$$

The two-dimensional (2D) anisotropy function,  $F(r, \theta)$ , quantifies the change in the dose rate distribution around the source as a function of  $\theta$  relative to that in the transverse plane at the same radial distance:

$$F(r, \theta) = \frac{\dot{D}(r, \theta)}{\dot{D}(r, \theta_0)} \frac{G_L(r, \theta_0)}{G_L(r, \theta)}. \quad (17)$$

In the case where a treatment planning system requires a one-dimensional (1D) dose distribution as input data, the following equation should be used:

$$\dot{D}(r) = S_K \cdot \Lambda \cdot \frac{G_X(r, \theta_0)}{G_X(r_0, \theta_0)} \cdot g_X(r) \cdot \phi_{\text{an}}(r), \quad (18)$$



where the quantities are the same as those defined above, except for the 1D anisotropy function,  $\phi_{\text{an}}(r)$ :

$$\phi_{\text{an}}(r) = \frac{\int_0^\pi \dot{D}(r, \theta) \sin(\theta) d\theta}{2\dot{D}(r, \theta_0)}. \quad (19)$$

The value of the 1D anisotropy function at a given radial distance  $r$  is the quotient of the solid-angle-weighted dose rate integrated over all space and the dose rate on the transverse plane.

**5.1.1. AAPM TG-43 recommendations: experimental techniques for dose measurement.** In order to calculate the TG-43 parameters defined above, the dose rate must be measured around the source in a tissue-equivalent phantom. The air-kerma strength of the source is determined either by a NIST measurement or by using an instrument (usually a well-ionization chamber) that has a NIST-traceable calibration. Of the various methods available for measuring the dose rate around a brachytherapy source in a phantom (i.e. miniature ionization chambers, diodes, radiochromic film, plastic scintillators, gels), LiF thermoluminescent dosimeters (TLDs) are recommended by TG-43U1. Various phantom materials are commercially available, the material composition of which may have to be experimentally verified. TLDs should be placed within a distance range of 0.5 cm to 7 cm for  $^{125}\text{I}$  sources, and 0.5 cm to 5 cm for  $^{103}\text{Pd}$  sources, allowing at least 5 cm to provide adequate backscatter. Angular data should be collected at a minimum of  $10^\circ$  increments.

**5.1.2. AAPM TG-43 recommendations: theoretical techniques for dose calculation.** Various Monte Carlo codes, such as EGS, MCNP and PTRAN, have been used to calculate the dose distribution from brachytherapy sources. It is important that modern cross-section libraries be used that are equivalent to the current NIST XCOM database (i.e. DLC-146 or EPDL97). Physical dimensions and elemental composition of the source capsule and internal components should be known as accurately as possible. For calculation of  $s_K$  (air-kerma strength per history), it is preferable to use a model of the WAFAC geometry as opposed to a point detector. This will allow a more meaningful comparison to be made between the calculated and measured dose rate constants. The recommended minimum distance and angular ranges are the same as those specified above for measurements, but it is typical of investigators to perform dose calculations at finer increments and a wider range of distances.

**5.1.3. AAPM TG-43 recommendations: determination of consensus dosimetry data sets.** Consensus dosimetry data sets are formed from at least one experimental and one theoretical data set. To be included, all data must be accepted for publication in a peer-reviewed scientific journal prior to a given date. The scientific methods used to obtain each candidate data set are critically evaluated, and in the case of experimental and theoretical data published in the same paper or by the same research group, the independence of results is verified. The consensus dose rate constant,  $_{\text{CON}}\Lambda$ , is calculated

as the average of the experimentally determined dose rate constant and the Monte Carlo calculated dose rate constant. In the case of having more than one experimental or theoretical value, these are averaged prior to calculating  $_{\text{CON}}\Lambda$ . In order to compare radial dose function and anisotropy function data, the use of the same geometry function is verified. If different geometry functions are used (usually due to different source effective lengths), the data sets are modified such that they all have the same  $G_X(r, \theta)$ . The consensus radial dose function,  $_{\text{CON}}g(r)$ , and the consensus anisotropy function,  $_{\text{CON}}F(r, \theta)$ , are chosen based on criteria such as resolution, range of distances covered and smoothness of data. Having a comprehensive analysis of uncertainty accompanying each candidate data set is important in evaluating the agreement between them.

## 5.2. Photon-emitting brachytherapy sources with average energy higher than 50 keV

**5.2.1. AAPM-ESTRO recommendations.** In 2007, the AAPM HEBD working group published dosimetric prerequisites for the use of brachytherapy sources that emit photons with an average energy greater than 50 keV (Li *et al* 2007). The recommendations given in this report are from the AAPM and the European Society of Therapeutic Radiology and Oncology (ESTRO), and apply to LDR, HDR and PDR sources. LDR sources include those containing the radionuclides  $^{137}\text{Cs}$  and  $^{192}\text{Ir}$ , and all HDR and PDR sources covered by this document contain  $^{192}\text{Ir}$ .

$^{137}\text{Cs}$  LDR brachytherapy sources, in the form of cylindrical tubes or needles, have been used clinically for many years. The results of dosimetric studies on these sources have generally been in good agreement, as the high energy of the emergent photons facilitates accurate dosimetry due to the absence of steep dose gradients and capsule attenuation effects as seen with low-energy sources. Therefore, this report recommends use of data sets previously referenced in the AAPM Task Group 56 report (Nath *et al* 1997).

For  $^{137}\text{Cs}$  and  $^{192}\text{Ir}$  source designs that are currently available commercially, one experimental and one theoretical Monte Carlo or analytical transport equation solution dosimetry study are recommended, except if the source has an encapsulation design similar to that of an existing model. In this case, one dosimetric study is sufficient. For LDR sources, measurement of the air-kerma strength should be traceable to the appropriate NIST standard. For HDR sources, a NIST standard is not currently available; however, several other primary standards laboratories do maintain such standards. In the US, calibrations of HDR  $^{192}\text{Ir}$  sources are performed by the AAPM ADCLs by means of an in-air measurement using ionization chambers with NIST-traceable calibration coefficients as described in section 3.2.2. The results of dose rate measurements and calculations should be presented using the TG-43 formalism as well as in the form of 'along-and-away' tables.

**5.2.2. GEC-ESTRO dosimetry data sets for LDR, HDR and PDR sources.** Dosimetry data sets for LDR, HDR and PDR



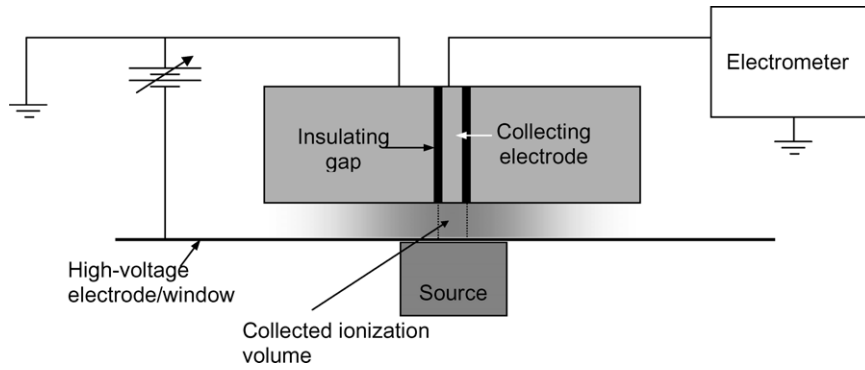


**Figure 9.** Schematic of a typical extrapolation chamber used to measure surface absorbed dose rate.

brachytherapy sources containing  $^{60}\text{Co}$ ,  $^{137}\text{Cs}$ ,  $^{192}\text{Ir}$  and  $^{169}\text{Yb}$  are available on the Universitat de Valencia (2008) web site. Descriptions of each source are included, as well as dosimetry data using both the AAPM TG-43 formalism and ‘along-and-away’ tables.

## 6. Primary standards for reference absorbed dose rate calibrations for beta particle radiation sources

### 6.1. General

Unlike photon brachytherapy source standards, beta particle brachytherapy standards realize the quantity absorbed dose to water or tissue. All primary standards for beta particle source dosimetry are based upon extrapolation ionization chambers, which are parallel plate ionization chambers whose volumes are continuously variable. A typical measurement geometry is shown in figure 9. The Bragg–Gray principle is used to convert ionization density (current per unit air volume) to absorbed dose rate to water,  $\dot{D}_w$ , according to the equation

$$\dot{D}_w = \frac{(\bar{W}/e)S_{w,a}}{\rho_{a0}A_{\text{eff}}} \left[ \frac{d}{d\ell} \Pi k' I(\ell) \right]_{\ell=0} \Pi k, \quad (20)$$

where  $(\bar{W}/e)$  is the quotient of the mean energy required to produce an ion pair in air and the elementary charge  $e$ , with a recommended value of  $33.97 \text{ J C}^{-1}$ .  $\rho_{a0}$  is the density of air at the reference conditions of temperature, pressure and relative humidity.  $A_{\text{eff}}$  is the effective area of the collecting electrode, which must be smaller than the source field size being measured.  $S_{w,a}$  is the ratio of the mean mass-electronic stopping powers in water to air.  $\Pi k$  is the product of the correction factors which are independent of the chamber depth and  $[(d/d\ell)\Pi k' I(\ell)]_{\ell=0}$  is the limiting value of the slope of the corrected current versus chamber depth,  $\ell$ , function, and  $\Pi k'$  is the product of the correction factors which vary with the chamber depth.

The quantity  $S_{w,a}$  is given by

$$S_{w,a} = \frac{\int_0^{E_{\text{max}}} (\Phi_E)_w (S/\rho)_{\text{el},w} dE}{\int_0^{E_{\text{max}}} (\Phi_E)_w (S/\rho)_{\text{el},a} dE}, \quad (21)$$

where  $(\Phi_E)_w$  is the spectrum of electrons at the reference point of the extrapolation chamber,  $(S/\rho)_{\text{el},w}$  is the mass-electronic stopping power for an electron with kinetic energy

$E$  in water and  $(S/\rho)_{\text{el},a}$  is the corresponding quantity for air. It is assumed that secondary electrons (delta rays) deposit their energy where they are generated so that they do not contribute to the electron fluence. The upper limit of the integrals is given by the maximum energy,  $E_{\text{max}}$ , of the beta radiation in the fluence spectrum and the lower limit corresponds to the lowest energy in the spectrum, here indicated by a zero. In principle this spectrum also includes any electrons set in motion by bremsstrahlung photons but these are usually of negligible importance.

Examples of corrections which are independent of chamber depth include a correction for the difference in backscatter between the collecting electrode material and water, and a correction for attenuation of beta particles in the entrance window of the extrapolation chamber. Corrections which are dependent on chamber depth include corrections for variations in ambient temperature and pressure to reference conditions, recombination, and the effect of beam divergence. These corrections are described in more detail in the following sections for the various primary standards covered in this paper.

### 6.2. NIST medical extrapolation chamber

The extrapolation chamber used at NIST as a primary standard for beta particle sources used for medical applications is based on a design by Loevinger (Loevinger and Trott 1966, Pruitt 1987). The unique feature of this extrapolation chamber is the ability to easily remove and replace the collecting electrode, allowing the same chamber to be used for multiple applications. Over the years a series of collecting electrodes have been built, which range in collecting diameter from approximately 1 mm up to 30 mm. These have allowed studies of the effect of collecting area on the linearity of the current versus chamber depth (extrapolation) function. The main feature of this function is a sublinearity at larger chamber depths, which occurs due to the effect of the extreme source field divergence at the source surface. To minimize this effect, measurements are performed at chamber depths as small as possible, usually between about  $50 \mu\text{m}$  and  $150 \mu\text{m}$ , and Monte Carlo based divergence corrections are applied.

For the measurement of planar beta particle sources at the source surface or at depth in water equivalent material, a collecting electrode with a 4 mm diameter is used (Soares 1991, 2004). In order to properly position this electrode at

**Table 2.** Uncertainty budget for calibration of beta particle planar sources with the NIST medical extrapolation chamber.

Component of uncertainty	$s_i/\%$	$u_j/\%$
Net current	0.1	0.1
Air density correction	—	0.1
Recombination correction	—	0.1
Divergence correction	0.5	—
Rate of change of current	2.6	2
Average energy per ion pair	—	0.15
Stopping power ratio	—	0.6
Backscatter correction	0.6	—
Collecting electrode area	0.6	—
Combined uncertainty (quadratic sum)	3.5	
Expanded uncertainty (combined $\times 2$ )	7	

the source centre, a mapping of the dose rate distribution at the source surface is first performed using a collecting electrode with a 1 mm diameter. From this distribution, the source centre is determined, and the 1 mm electrode is replaced with the 4 mm electrode. The NIST medical extrapolation chamber is different from most other extrapolation chambers because the collecting electrode position remains fixed and the high-voltage electrode/entrance window is moved during the determination of the extrapolation function. Because of this, to keep a constant distance between the source and the entrance window, the source must also be moved when the chamber depth is changed. To do this, as well as to move the source in the plane parallel to the entrance window during the source mapping process, a three-dimensional positioning system is employed. A fourth motor controls the changing of the chamber depth.

For beta particle seed and line sources, the 1 mm electrode is used to measure absorbed dose rate at the surface of tissue-equivalent phantoms in which the sources are placed (Soares *et al* 1998). Although a range of phantom blocks have been made over the years, most often the sources are measured at the reference depth of 2 mm. As with the planar sources, the dose distribution on the block surface is first mapped with the 1 mm collecting electrode to determine the central point of the dose distribution where the extrapolation measurement will take place.

The combined, expanded uncertainty of the calibration of planar sources is estimated to be  $\pm 7\%$  (see table 2). The random uncertainty components are calculated as standard deviations of the mean of replicate readings; other components are estimated so that they can be assumed to have the approximate character of standard deviations. The combined, expanded uncertainty is two times the square root of the quadratic sum of all the component uncertainties; it is considered to have the approximate significance of a 95% confidence limit. For seed and line sources, the combined expanded uncertainty is  $\pm 10\%$  (see table 3).

### 6.3. PTB medical extrapolation chamber

PTB was one of the pioneers in the standardization of reference radiation fields used for radiation protection, and the primary standard extrapolation chamber still used by virtually all

**Table 3.** Uncertainty budget for calibration of beta particle seed and line sources with the NIST medical extrapolation chamber.

Component of uncertainty	$s_i/\%$	$u_j/\%$
Net current	0.2	0.1
Air density correction	—	0.1
Recombination correction	—	0.1
Divergence correction	0.5	—
Rate of change of current	2.6	3
Average energy per ion pair	—	0.15
Stopping power ratio	—	0.6
Backscatter correction	0.6	—
Collecting electrode area	2.9	—
Combined uncertainty (quadratic sum)	5	
Expanded uncertainty (combined $\times 2$ )	10	

laboratories for this application was developed there. A modification of this extrapolation chamber (changing the 30 mm diameter collecting electrode to a 10 mm diameter electrode) is used at PTB for surface and near surface measurements of planar beta particle sources (Selbach 2002). The main use of this standard was to characterize a HDR secondary standard  $^{90}\text{Sr}/\text{Y}$  source at a number of different depths which would be used to transfer PTB standards (Selbach and Soares 2003), in analogy the very successful Beta Secondary Standard set of sources that are used worldwide for realizing reference radiation fields for radiation protection. The use of this 10 mm collecting electrode extrapolation chamber, however, has been superseded by the multi-electrode extrapolation chamber described below.

### 6.4. PTB multi-electrode extrapolation chamber

The primary standard of PTB is a novel extrapolation chamber based on a newly designed multi-electrode extrapolation chamber (MEC) which meets the requirements of high spatial resolution and small uncertainty in measurement (Bambynek 2002). In contrast to a conventional extrapolation chamber, the central part of the MEC is a segmented collecting electrode which was manufactured in the clean room fabrication centre of PTB by means of electron beam lithography on a wafer. A large number (thirty or more) collecting electrodes 1 mm  $\times$  1 mm in size are arranged in the centre of the wafer. A precise displacement device consisting of three piezoelectric macro-translators changes the chamber depth by moving the wafer collecting electrode relative to the fixed entrance window. An upper estimation of the relative expanded uncertainty ( $k = 2$ ) of the absorbed dose rate to water at a depth of 2 mm in water-equivalent material is 6.0%.

### 6.5. NMI extrapolation chamber

The beta radiation source standard extrapolation chamber of the Netherlands Meetinstituut (NMI) is of a design similar to the NIST extrapolation chamber (van der Marel and Van Dijk 2003). The collecting electrode remains stationary while the entrance window is moved to change the collecting volume, and a precision three-dimensional stage moves the source to allow centering, field mapping and maintenance of the position

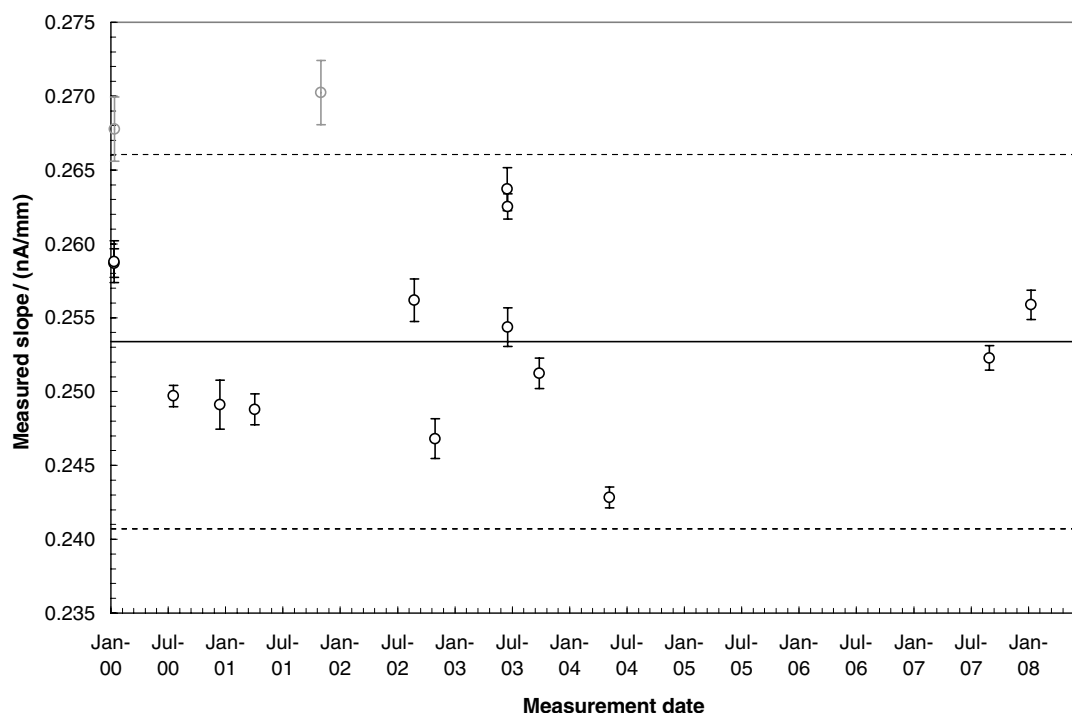


**Figure 10.** Calibration history (since 2000) of the NIST reference ophthalmic applicator. The dashed lines indicate the acceptance criteria for an acceptable measurement. The standard deviation of all acceptable measurements shown is 2.3%.

relative to the entrance electrode as the volume is changed. The collecting electrode is 1 mm in diameter, constructed from D400 water-equivalent plastic. A relative expanded uncertainty of 11% ( $k = 2$ ) has been assigned to the calibration of planar sources.

## 7. Transfer and maintenance of absorbed dose rate standards for beta particle brachytherapy sources

### 7.1. Quality assurance techniques in calibrations of beta particle sources

As with photon brachytherapy sources, secondary standard sources are calibrated with the primary standards and used to transfer calibrations. Such secondary standards can also serve as quality control checks on the constancy of the primary standard. At NIST, to verify that the extrapolation chamber is operating properly, a secondary standard source (either planar or linear) is first recalibrated and the measurement compared with previous calibrations. The results of this calibration must be within  $\pm 5\%$  of the decay corrected average of all previous valid measurements before the unknown source can be measured. A control chart showing all measurements of the reference source since 2000 is shown in figure 10. In addition, this secondary standard source may be used to calibrate other detection systems, such as radiochromic film, for use in additional measurements on the unknown source. At NIST, such calibrated film is used for detailed high resolution maps of the surface dose rate distribution of sources under calibration. Such a two-dimensional MQA system is shown in figure 11.

### 7.2. Transfer of standards to secondary calibration laboratories, source manufacturers and clinics

Secondary standard sources such as those described in the previous paragraph may be used by secondary standard laboratories or users as local standards. In the US, such a NIST-calibrated secondary standard is used by the UWADCL to calibrate detectors (radiochromic film) used to calibrate customer sources. Similarly, for beta particle seed and line sources, NIST-calibrated line sources are used to calibrate well-ionization chambers which then serve as local standards at secondary laboratories.

### 7.3. International comparisons

There have not been a great deal of dosimetry comparisons between primary standards laboratories for medical beta particle sources, mainly because up until recently only NIST maintained such standards. The first modern comparison of calibrations was performed in 1996 to 1997 using planar  $^{90}\text{Sr/Y}$  and  $^{106}\text{Ru/Rh}$  sources (Soares *et al* 2001). The participants included primary standard laboratories (NIST and NPL), secondary laboratories and clinical users. The results of this comparison indicated agreement among participants at the level of about 10% ( $k = 1$ ) for measurements of planar sources at a depth of 1 mm.

The first formal comparison between primary standard laboratories took place in 2001 between PTB and NIST using a PTB supplied planar  $^{90}\text{Sr/Y}$  source. Although never published, agreement between the two laboratories was within 5%. In 2005 an informal comparison of surface dose rate from the NIST reference line source was completed between NIST and NMI. The results of this comparison indicated very good

	National Standard: Extrapolation chamber with 4 mm electrode	Additional Device: Calibrated Radiochromic Film
Unknown Source	Calibration	Quality Control on Calibration
Reference Eye Plaque	Quality Control on Standard	Calibration of Radiochromic Film

**Figure 11.** Two-dimensional MQA model applied to the calibration of ophthalmic applicators.

agreement between the measured slopes of the current versus chamber depth functions, although reported dose rates differed by about 10%, mainly due to the use of different values for various corrections. A similar comparison using the PTB reference line source was performed between PTB and NIST in 2006, which indicated agreement in reported surface absorbed dose rates within 4% (Bambynek and Soares 2007). Currently (2008), there is an ongoing comparison of surface absorbed dose rates for planar  $^{106}\text{Ru}/\text{Rh}$  sources between PTB and NIST using a PTB reference planar source.

## 8. Dosimetry protocols for medical applications of beta particle sources

The first formal protocols for beta particle brachytherapy calibrations involved intravascular brachytherapy. The first published protocol was AAPM TG 60 (Nath *et al* 1999) which proposed a modified TG-43 formalism for linear arrays of seed sources. The main difference from the TG-43 protocol is the replacement of the  $S_K\Lambda$  term with the reference absorbed dose rate in water at a distance of 2 mm in water. These recommendations were extended by a German Medical Physics Society (DGMP) Working Group which published its report 18 in 2001, again covering only seed and line sources (DGMP 2001). Clinical parameters for seed and line sources were better defined in an EVA GEC ESTRO document also published in 2001 (Pötter *et al* 2001). A year later, the International Atomic Energy Agency (IAEA) published TECDOC 1274 which gave calibration and measurement guidance for both planar as well as seed and line sources (IAEA 2002). However, all these documents had access to drafts of an International Commission on Radiation Units and Measurements (ICRU) report which was begun in 1996 and which covered medical applications of beta radiation (ICRU 2004). This document was delayed because of the rise (and fall) of the field of intravascular brachytherapy, and by the decision to include not only this application, but also low-energy photon brachytherapy sources used to treat ocular melanoma. This ICRU Report Number 72, which contains the first formalisms for the dosimetry of planar beta particle sources as well, was finally published in 2004. In the same year, the Netherlands Commission on Radiation Dosimetry (NCS) published a document which extended and clarified

some of the definitions in ICRU 72, and which also addressed the breakdown of the TG-43/60 formalism for beta particle line sources which are longer than the range of beta particles in water (Kollaard *et al* 2004). These formalisms were adopted in the work of AAPM TG-149, which published a complete set of consensus data to be used with the new formalisms in 2007 (Chiu-Tsao *et al* 2007). Currently there is an ISO standard in the final stages of approval which synthesizes all of the above work and which gives guidance for clinical dosimetry for all types of beta particle radiation sources (ISO 2008).

## 9. Prospects for future absorbed dose to water standards for photon brachytherapy sources

The dosimetry of photon brachytherapy sources is currently based on air-kerma rate values at 1 m. However, for clinical applications, the relevant quantity is the absorbed dose rate to water at short distances (1 cm typically) in water. Conversions between air-kerma and dose are done by the dose rate constant (Rivard *et al* 2004a, 2004b):

$$\Lambda = \frac{\dot{D}(r_0, \theta_0)}{S_K}, \quad (22)$$

where  $\dot{D}(r_0, \theta_0)$  denotes the absorbed dose rate to water at the reference position and  $S_K$  is the air-kerma strength (or RAKR). Presently, the determination of  $\Lambda$  relies on Monte Carlo simulations or relative measurements performed with passive dosimeters and therefore is affected by a large relative uncertainty (greater than 5%).

Recently, several European national laboratories have decided to join their efforts in order to establish direct measurements of absorbed dose to water at clinically relevant distances from HDR brachytherapy sources. With the support of the European Union, a set of independent experimental devices are currently under development (water and graphite calorimeters). Within three years, they should be able to provide some direct measurements of the absorbed dose rate to water in the vicinity of HDR brachytherapy sources with much lower uncertainties than are currently available. Parallel to this effort, work is also proceeding on absorbed dose to water standards for LDR brachytherapy sources.



## References

- Attix F H 1984 Determination of  $A_{\text{ion}}$  and  $P_{\text{ion}}$  in the new AAPM radiotherapy dosimetry protocol *Med. Phys.* **11** 714–16
- Baker M, Bass G A and Woods M J 2002 Calibration of the NPL secondary standard radionuclide calibrator for I-125 seeds used for prostate brachytherapy *Appl. Radiat. Isot.* **56** 321–25
- Bambynek M 2002 Development of a multi-electrode extrapolation chamber as a prototype of a primary standard for the realization of the quantity of the absorbed dose to water for beta radiation brachytherapy sources *Nucl. Instrum. Methods A* **492** 264–75
- Bambynek M and Soares C G 2007 Intercomparison of primary standards at PTB and NIST for the realization of the unit of absorbed dose to water for beta particle brachytherapy sources *Med. Phys.* **34** 2463
- Bielajew A F 1990 Correction factors for thick-walled ionisation chambers in point-source photon beams *Phys. Med. Biol.* **35** 501–16
- Boag J W 1987 *The Dosimetry of Ionizing Radiation* vol 2 K R Kase *et al* (New York: Academic) 169–243
- Borg J, Kawrakow I, Rogers D W O and Seuntjens J P 2000 Monte Carlo study of correction factors for Spencer-Attix cavity theory at photon energy at or above 100 keV *Med. Phys.* **27** 1804–13
- Borg J and Rogers D W O 1999 Spectra and air-kerma strength for encapsulated  $^{192}\text{Ir}$  sources *Med. Phys.* **26** 2441–4
- Büermann L, Kramer H M and Selbach, H-J 1995 Reference air kerma rate determination of an iridium-192 brachytherapy source *Nucletron-Oldelft Activity Report No 7*, S. pp 43–7
- Chiu-Tsao S-T, Schaart D R, Soares C G and Nath R 2007 Dose calculation formalisms and consensus dosimetry parameters for intravascular brachytherapy dosimetry: recommendations of the AAPM Therapy Physics Committee Task Group No. 149 *Med. Phys.* **34** 4126–57
- Culbertson W S, DeWerd L A, Anderson D R and Micka J A 2006 Large-volume ionization chamber with variable apertures for air-kerma measurements of low-energy radiation sources *Rev. Sci. Instrum.* **77** 015105
- Decay Data Evaluation Project (DDEP) 2004 LNE-CEA/LNHB (France), PTB (Germany), INEEL (USA), KRI (Russia), LBNL (USA), NPL (UK), CIEMAT (Spain) and <http://www.nucleide.org/DDEP.htm>
- DeWerd L A, Huq M S, Das I J, Ibbott G S, Hanson W F, Slowey T W, Williamson J F and Coursey B M 2004 Procedures for establishing and maintaining consistent air-kerma strength standards for low-energy, photon-emitting brachytherapy sources: recommendations of the Calibration Laboratory Accreditation Subcommittee of the American Association of Physicists in Medicine *Med. Phys.* **31** 675–81
- Deutsche Gesellschaft für Medizinische Physik (DGMP) 2001 *Guideline for Medical Physical Aspects of Intravascular Brachytherapy*, DGMP Report No. 16 ed U Quast, T W Kaulich and D Fluhs (DGMP, Cologne) <http://www.dgmp.de> (pdf-file)
- Douysset G, Gouriou J, Delaunay F, DeWerd L, Stump K and Micka J 2005 Comparison of dosimetric standards of USA and France for HDR brachytherapy *Phys. Med. Biol.* **50** 1961–78
- Douysset G, Ostrowsky A and Delaunay F 2008a Some unexpected features of PTW/Nucletron well-type ionisation chambers *Phys. Med. Biol.* **53** N269–75
- Douysset G, Sander T, Gouriou J and Nutbrown R 2008b Comparison of air kerma standards of LNE-LNHB and NPL for  $^{192}\text{Ir}$  HDR brachytherapy sources: EUROMET Project No. 814 *Phys. Med. Biol.* **53** N85–97
- European Society for Therapeutic Radiology and Oncology (ESTRO) 2004 *A Practical Guide to Quality Control of Brachytherapy Equipment* ed J Venselaar and J P Pérez-Calatayud Booklet No. 8, ISBN 90-804532-8
- Goetsch S J, Attix F H, Pearson D W and Thomadsen B R 1991 Calibration of  $^{192}\text{Ir}$  high-dose-rate afterloading systems *Med. Phys.* **18** 462–7
- Goetsch S J, Attix F H, DeWerd L A and Thomadsen B R 1992 A new re-entrant ionization chamber for the calibration of iridium-192 high dose rate sources *Int. J. Radiat. Oncol. Biol. Phys.* **24** 167–70
- International Atomic Energy Agency (IAEA) 1999 Calibration of brachytherapy sources. Guidelines of standardized procedures for the calibration of brachytherapy sources at secondary standard dosimetry laboratories (SSDLs) and hospitals *TECDOC-1079* Vienna
- International Atomic Energy Agency (IAEA) 2002 Calibration of photon and beta-ray sources used in brachytherapy *TECDOC-1274* Vienna
- International Commission on Radiation Units and Measurements (ICRU) 1985 Dose and volume specification for reporting intracavitary therapy in gynaecology *ICRU Report No 38* (Washington, DC: ICRU)
- International Commission on Radiation Units and Measurements (ICRU) 1997 Dose and volume specification for reporting interstitial therapy *ICRU Report No 58* (Bethesda, MD: ICRU)
- International Commission on Radiation Units and Measurements (ICRU) 2004 Dosimetry of beta ray sources and low energy photon brachytherapy sources *ICRU Report No 72* (Bethesda, MD: ICRU)
- International Organization for Standardization (ISO) 2008 Clinical Dosimetry—Beta radiation sources for brachytherapy *ISO/DIS 21439* (Geneva, Switzerland: ISO)
- Kollaard R P, Dries W J F, van Kleffens H J, Aalbers A H L, van der Marel J, Marijnissen J P A, Piessens M, Schaart D R and de Vroome H 2004 Quality control of sealed brachytherapy sources in brachytherapy *NCS Report 14*, Netherlands Commission on Radiation Dosimetry
- Kondo S and Randolph M L 1960 Effect of finite size of ionization chambers on measurement of small photon sources *Rad. Res.* **13** 37–60
- Kutcher G J *et al* 1994 Comprehensive QA for radiation: Report of AAPM Radiation Therapy Committee Task Group No. 40 *Med. Phys.* **21** 581–618
- Li Z, Das R K, DeWerd L A, Ibbott G S, Meigooni A S, Pérez-Calatayud J, Rivard M J, Sloboda R S and Williamson J F 2007 Dosimetric prerequisites for routine clinical use of photon emitting brachytherapy sources with average energy higher than 50 keV *Med. Phys.* **34** 37–40
- Loevinger R and Trott N G 1966 Design and operation of an extrapolation chamber with removable electrodes *Int. J. Appl. Radiat. Isot.* **17** 103–11
- Loftus T P 1970 Standardization of cesium-137 gamma-ray sources in terms of exposure units (Roentgens) *J. Res. Natl Bur. Stand. A* **74** 1–6
- Loftus T P 1980 Standardization of iridium-192 gamma-ray sources in terms of exposure *J. Res. Natl Bur. Stand.* **85** 19–25
- Mainegra-Hing E and Rogers D W O 2006 On the accuracy of techniques for obtaining the calibration coefficient  $N_K$  of  $^{192}\text{Ir}$  HDR brachytherapy sources *Med. Phys.* **33** 3340–6
- Mitch M G, Lamperti P J, Seltzer S M and Coursey B M 2002 New methods for anisotropy characterization of Pd-103 and I-125 prostate brachytherapy seed emissions using radiochromic film and angular x-ray spectrometry *Med. Phys.* **29** 1228
- Nath R, Anderson L L, Luxton G, Weaver K A, Williamson J F and Meigooni A S 1995 Dosimetry of interstitial brachytherapy sources: Recommendations of the AAPM Radiation Therapy Committee Task Group No. 43 *Med. Phys.* **22** 209–34
- Nath R, Anderson L L, Meli J A, Olch A J, Stitt J A and Williamson J F 1997 Code of Practice for brachytherapy physics: Report of the AAPM Radiation Therapy Committee Task Group No. 56 *Med. Phys.* **24** 1557–98



- Nath R *et al* 1999 Intravascular brachytherapy physics: Report of the AAPM Radiation Therapy Committee Task Group No. 60 *Med. Phys.* **26** 19–152
- Podgorsak M B, DeWerd L A, Thomadsen B R and Paliwal B R 1992 Thermal and scatter effects on the radiation sensitivity of well chambers used for high dose rate  $^{192}\text{Ir}$  calibrations *Med. Phys.* **19** 1311–4
- Poirier A and Douysset G 2006 Influence of ambient humidity on the current delivered by air-vented ionization chambers revisited *Phys. Med. Biol.* **51** 4995–5006
- Pötter R *et al* (ed) 2001 EVA GEC ESTRO Recommendations: recording, reporting, quality assurance, education, and training in endovascular brachytherapy. Recommendations of the Endovascular GEC-ESTRO Working Group EVA GEC-ESTRO. *Radiother. Oncol.* **59** 339–60
- Pruitt J S 1987 *Calibration of Beta-Particle-Emitting Ophthalmic Applicators* NBS Special Publication 250–9 (Gaithersburg: NBS)
- Rivard M J, Coursey B M, DeWerd L A, Hanson W F, Huq M S, Ibbott G S, Mitch M G, Nath R and Williamson J F 2004a Update of AAPM Task Group No 43 Report: a revised AAPM protocol for brachytherapy dose calculations (AAPM Report No 84) *Med. Phys.* **31** 633–74
- Rivard M J, Butler W M, DeWerd L A, Huq M S, Ibbott G S, Li Z, Mitch M G, Nath R and Williamson J F 2004b Update of AAPM Task Group No. 43 Report: A revised AAPM protocol for brachytherapy dose calculations *Med. Phys.* **31** 3532–3 (erratum)
- Rivard M J, Butler W M, DeWerd L A, Huq M S, Ibbott G S, Meigooni A S, Melhus C S, Mitch M G, Nath R and Williamson J F 2007 Supplement to the 2004 update of the AAPM Task Group No. 43 Report *Med. Phys.* **34** 2187–205
- Rossiter M J, Williams T T and Bass G A 1991 Air kerma rate calibration of small sources of Co-60, Cs-137, Ra-226 and Ir-192 *Phys. Med. Biol.* **36** 279–84
- Sander T and Nutbrown R F 2006 The NPL air kerma primary standard TH100C for high dose rate  $^{192}\text{Ir}$  brachytherapy sources *NPL Report DQL-RD 004* ISSN 1744-0637, Teddington UK (available at [publications.npl.co.uk](http://publications.npl.co.uk))
- Selbach H-J 2002 The PTB secondary standard for intravascular brachytherapy *Med. Phys.* **29** 1226
- Selbach H-J 2006 Neue Kalibrieranlage für  $^{192}\text{Ir}$ - und  $^{60}\text{Co}$ -Brachytherapie-Strahlungsquellen *Tagungsband der 37. Jahrestagung der Deutschen Gesellschaft für Medizinische Physik (DGMP)*, Regensburg, 244
- Selbach H-J and Büermann L 2004 Vergleich zweier Verfahren zur Darstellung der Einheit der Kennosisleistung für  $^{192}\text{Ir}$ -HDR-Brachytherapiequellen *Tagungsband der 35. Jahrestagung der Deutschen Gesellschaft für Medizinische Physik (DGMP)*, Leipzig, 82
- Selbach H-J, Kramer H-M and Culbertson W S 2008 Realization of reference air-kerma rate for low-energy photon sources *Metrologia* **45** 422–8
- Selbach H-J and Soares C G 2003 New developments on primary standards for brachytherapy at NIST (US) and PTB (Germany) *Proc. Int. Symp. Standards and Codes of Practice in Medical Radiation Dosimetry* (Vienna: IAEA) pp 101–10 ISBN 0074-1884
- Seltzer S M and Bergstrom P M 2003 Changes in the U.S. primary standards for the air kerma from gamma-ray beams *J. Res. Natl Inst. Stand. Technol.* **108** 359–81
- Seltzer S M, Lamperti P J, Loevinger R, Mitch M G, Weaver J T and Coursey B M 2003 New national air-kerma-strength standards for I-125 and Pd-103 brachytherapy seeds *J. Res. Natl Inst. Stand. Technol.* **108** 337–58
- Selvam T P, Govinda Rajan K N, Sethulakshmi P and Bhatt B C 2001 Monte Carlo aided room scatter studies in the primary air kerma strength standardization of a remote afterloading  $^{192}\text{Ir}$  HDR source *Phys. Med. Biol.* **46** 2299–315
- Septon J P, Woods M J, Rossiter M J, Williams T T, Dean J C J, Bass G A and Lucas S E M 1993 Calibration of the NPL secondary standard radionuclide calibrator for Ir-192 brachytherapy sources *Phys. Med. Biol.* **38** 1157–64
- Soares C G 1991 Calibration of ophthalmic applicators at NIST—a revised approach *Med. Phys.* **18** 787–93
- Soares C G 2004 Calibration of ophthalmic applicators, NIST Quality Manual, Ionizing Radiation Division QM-II, Procedure 9 <http://physics.nist.gov/Divisions/Div846/QualMan/Procedures/WebProcedure09v200.pdf>
- Soares C G, Halpern D and Wang C-K 1998 Calibration and Characterization of Beta-Particle Sources for Intravascular Brachytherapy *Med. Phys.* **25** 339–46
- Soares C G, Vynckier S, Järvinen H, Cross W G, Hokkanen J, Sipilä P, Flühs D, Schaeken B, Mourtada F A, Bass G A and Williams T T 2001 Dosimetry of beta-ray ophthalmic applicators: Comparison of different measurement methods *Med. Phys.* **28** 1373–84
- Stump K E, DeWerd L A, Micka J A and Anderson D R 2002 Calibration of new high dose rate  $^{192}\text{Ir}$  sources *Med. Phys.* **29** 1483–8
- Universitat de Valencia 2008 <http://www.uv.es/braphyqs/>
- van der Marel J and Van Dijk E 2003 Development of a Dutch primary standard for beta emitting brachytherapy sources *Standards and Codes of Practice in Medical Radiation Dosimetry, Proc. Int. Symp. Standards and Codes of Practice in Medical Radiation Dosimetry* (Vienna: IAEA) pp 93–100 ISBN 0074-1884
- Van Dijk E 2003 Comparison of two different methods to determine the air kerma calibration factor  $N_K$  for  $^{192}\text{Ir}$  *Proc. Int. Symp. Standards and Codes of Practice in Medical Radiation Dosimetry* (Vienna: IAEA) pp 129–36 ISBN 0074-1884
- Verhaegen F, Van Dijk E, Thierens H, Aalbers A and Seuntjens J 1992 Calibration of low activity  $^{192}\text{Ir}$  brachytherapy sources in terms of reference air-kerma rate with large volume spherical ionisation chambers *Phys. Med. Biol.* **37** 2071–82